

IOWA STATE UNIVERSITY

Digital Repository

Retrospective Theses and Dissertations

Iowa State University Capstones, Theses and
Dissertations

1961

The effect of oxygen on physical and mechanical properties of vanadium

Samuel Arthur Bradford

Iowa State University

Follow this and additional works at: <https://lib.dr.iastate.edu/rtd>



Part of the [Metallurgy Commons](#)

Recommended Citation

Bradford, Samuel Arthur, "The effect of oxygen on physical and mechanical properties of vanadium " (1961). *Retrospective Theses and Dissertations*. 2454.

<https://lib.dr.iastate.edu/rtd/2454>

This Dissertation is brought to you for free and open access by the Iowa State University Capstones, Theses and Dissertations at Iowa State University Digital Repository. It has been accepted for inclusion in Retrospective Theses and Dissertations by an authorized administrator of Iowa State University Digital Repository. For more information, please contact digirep@iastate.edu.

This dissertation has been 61-6155
microfilmed exactly as received

BRADFORD, Samuel Arthur, 1928-
THE EFFECT OF OXYGEN ON PHYSICAL AND
MECHANICAL PROPERTIES OF VANADIUM.

Iowa State University of Science and Technology
Ph.D., 1961
Engineering, metallurgy

University Microfilms, Inc., Ann Arbor, Michigan

THE EFFECT OF OXYGEN ON PHYSICAL AND MECHANICAL
PROPERTIES OF VANADIUM

by

Samuel Arthur Bradford

A Dissertation Submitted to the
Graduate Faculty in Partial Fulfillment of
The Requirements for the Degree of
DOCTOR OF PHILOSOPHY

Major Subject: Metallurgy

Approved:

Signature was redacted for privacy.

In Charge of Major Work

Signature was redacted for privacy.

Head of Major Department

Signature was redacted for privacy.

Dean of Graduate College

Iowa State University
Of Science and Technology
Ames, Iowa

1961

TABLE OF CONTENTS

	Page
I. INTRODUCTION	1
II. LITERATURE SURVEY	3
A. Lattice Constant	3
B. Solubility Limits of Interstitials	5
C. Hardness and Work Hardening	7
D. Embrittlement	8
E. Tensile Properties	8
F. Diffusion of Interstitials	9
G. Current Theories of Strain Aging	11
III. MATERIALS	16
A. Vanadium Metal	16
B. Sample Preparation	18
IV. APPARATUS AND EXPERIMENTAL METHODS	20
A. Lattice Constant Determination	20
B. Hardness Measurements	21
C. Bend Test Apparatus	21
D. Tensile Test Apparatus	23
V. PRESENTATION AND INTERPRETATION OF EXPERIMENTAL RESULTS	25
A. Lattice Constant Results	25
B. Hardness, Work Hardening, and Microstructure	27
C. Results of Bend Tests	29
D. Results of Tensile Tests	40
VI. DISCUSSION OF RESULTS	59
A. The Lattice Constant	59
B. Mechanical Strength and Embrittlement	61
C. Strain Aging	62
VII. SUMMARY AND CONCLUSIONS	68
VIII. BIBLIOGRAPHY	69
IX. ACKNOWLEDGMENTS	73

LIST OF TABLES

	Page
1. Typical analysis of vacuum-annealed crystal-bar vanadium	16
2. Lattice constant of vanadium at various oxygen concentrations	25
3. Bend tests of vanadium containing 150 ppm oxygen	31
4. Bend tests of vanadium containing 490 ppm oxygen	31
5. Bend tests of vanadium containing 700 ppm oxygen	31
6. Bend tests of vanadium containing 840 ppm oxygen	32
7. Bend tests of vanadium containing 1050 ppm oxygen	32
8. Bend tests of vanadium containing 1180 ppm oxygen	32
9. Bend tests of vanadium containing 1300 ppm oxygen	33
10. Bend tests of vanadium containing 1320 ppm oxygen	33
11. Bend tests of vanadium containing 1420 ppm oxygen	33
12. Bend tests of vanadium containing 1605 ppm oxygen	34
13. Bend tests of vanadium containing 1690 ppm oxygen	34
14. Bend tests of vanadium containing 1705 ppm oxygen	34
15. Bend tests of vanadium containing 1850 ppm oxygen	35
16. Bend tests of vanadium containing over 2500 ppm oxygen	35
17. Brittle-ductile transition temperatures of vanadium from bend tests	40
18. Tensile properties of vanadium containing 47 ppm oxygen	42
19. Tensile properties of vanadium containing 150 ppm oxygen	42
20. Tensile properties of vanadium containing 265 ppm oxygen	43
21. Tensile properties of vanadium containing 955 ppm oxygen	43
22. Tensile properties of vanadium containing 1800 ppm oxygen	44
23. Aging treatments from tensile test yield point return (all experiments performed on the same sample of vanadium containing 265 ppm oxygen)	46

LIST OF FIGURES

	Page
1. Tensile test specimen	19
2. Low-temperature bend test apparatus	22
3. Tensile test chamber	24
4. Effect of oxygen on the lattice constant of vanadium at 25°C	26
5. Effect of oxygen on the hardness of vanadium	28
6. Work hardening of vanadium	30
7. Effect of temperature and oxygen on the yield load in bend tests	36
8. Effect of temperature and oxygen on the maximum bending load	37
9. Effect of oxygen on the brittle-ductile transition of vanadium	39
10. Effect of oxygen on tensile properties at room temperature	48
11. Relation of hardness and tensile stress at maximum load	49
12. Strain hardening and elongation at room temperature	50
13. Variation of tensile strength with temperature	51
14. Variation of yield stress with temperature for low-oxygen vanadium	52
15. Variation of yield stress with temperature for high-oxygen vanadium	53
16. Effect of temperature on strain hardening of vanadium	54
17. Strain rate sensitivity of vanadium containing 265 ppm oxygen	55
18. Typical stress-strain curves	56
19. Serrations of tensile tests	57
20. Activation energy for return of yield point	58

I. INTRODUCTION

The widespread interest in the properties of vanadium has grown from the developments in refining methods for the metal. Until recently dismissed as "the hardest of all metals" (26), vanadium is now known to be quite ductile, even soft, when pure. At the present time consideration is being given to the use of vanadium in nuclear engineering as a fuel element cladding material because of its fairly low thermal neutron absorption and its good liquid-metal corrosion resistance. The formation of the stable oxides VO and V_2O_3 , rather than unstable V_2O_5 , in the presence of liquid sodium makes possible the use of vanadium in breeder reactors operating as high as 800°C (46). It also has possible uses in bonding of dissimilar metals and as a high-temperature structural material where its low thermal expansion might be of importance.

Having a body-centered cubic structure, vanadium is greatly affected by the presence of small amounts of impurities, particularly the interstitial atoms of oxygen, nitrogen, hydrogen, and carbon. Purification of calcium-reduced vanadium by the iodide crystal-bar process still leaves approximately 0.01% each of oxygen and carbon. Of the two, oxygen is generally considered to have a much greater effect on the mechanical properties, although no thorough study has been made of either impurity. Consequently, an examination of the effect of oxygen on the properties of vanadium would appear to be of considerable importance.

The areas selected for this study were:

1. The effect on the basic structure of vanadium by the introduction of oxygen, as shown by the change in lattice constant.
2. The variation in the mechanical properties of hardness, work hardening, strength, ductility, and the brittle-ductile transition temperature with oxygen content.
3. The strain aging of vanadium.

II. LITERATURE SURVEY

Prior to the determination of the effect of interstitial elements on the lattice constant of a metal it is important to know that the solubility limit is not exceeded, because a second phase will not affect the lattice constant if present in small amounts. For this reason it was necessary to find the work that has been published on the lattice constant of vanadium and the studies of solubility of the interstitial elements oxygen, nitrogen, carbon, and hydrogen in vanadium.

The mechanical properties of interest were the hardness, work hardening, the brittle-ductile transition, and the tensile properties above room temperature. Because strain aging is believed to be related to the diffusion of interstitials, it appeared advisable to investigate not only the present theories of strain aging but also the measurements that have been made of the diffusion of interstitial elements in vanadium.

A. Lattice Constant

Until recently very little confidence could be put in the published values of the lattice constant of vanadium because of the low purity of the metal. The accepted value has generally been 3.034 \AA (47), although compilations of the best lattice constant data have also listed 3.039 \AA (29) and 3.0338 kX , which is 3.0399 \AA (3).

A tetragonal distortion of the body-centered cubic lattice of vanadium caused by the solution of oxygen in vanadium, similar to that

of carbon in martensite, was reported by Klemm and Grimm (24). With vanadium 99.1% pure they obtained a lattice constant of 3.039 ± 0.003 Å. Addition of 1000 ppm oxygen changed the lattice to body-centered tetragonal with $a = 2.99$ Å and $c = 3.30$ Å approximately. For 2000 ppm oxygen they reported parameters of $a = 2.94$ Å and $c = 3.53$ Å. Rostoker *et al.* (40), however, found no evidence of any tetragonal distortion in α vanadium.

The first precise measurements of iodide crystal-bar vanadium were made by Neuburger (34), using an x-ray powder method to get a parameter of 3.0338 ± 0.0003 Å, and by Ketelaar (22), who found a value of $a_0 = 3.025$ Å.

The lattice constant of iodide vanadium, 99.34 \pm .3% pure, containing 120 ppm oxygen and 80 ppm nitrogen, has been measured by Seybolt and Sumsion (45) with a back-reflection focusing camera to get a value of 3.0255 ± 0.0005 Å using only lines of the (321) planes, or 3.0258 ± 0.0001 Å by Cohen's extrapolation. They found calcium-reduced vanadium containing 1400 ppm oxygen to have a lattice constant of 3.0275 Å. Essentially the same method was used by Beatty (4), who got a value of 3.0282 ± 0.0001 Å for iodide vanadium with 380 ppm oxygen and 210 ppm nitrogen.

Jordan and Duwez (21) measured the lattice of vanadium, purity not stated, with a powder camera and obtained a constant of 3.034 kX, or 3.041 Å.

Gurevich and Ormont (17) hammered a rod of calcium-reduced, "spectroscopically pure" vanadium and mounted it in a Debye-Scherrer type of camera. Annealing was omitted after working the metal to prevent oxygen contamination, and, admittedly, this gave broad, diffuse lines.

The lattice constant of pure vanadium was found to be 3.024 ± 0.001 Å. An addition of 390 ppm oxygen increased the value to 3.0255 Å.

Using a Geiger counter diffractometer, Loomis and Carlson (27) found a lattice constant of 3.0218 Å at 23°C for crystal-bar vanadium with less than 100 ppm oxygen. Recalculation of their data by Cohen's least-squares treatment gives a value of 3.0228 Å.

James and Straumanis (20) have reported a lattice constant of 3.0240 ± 0.0003 Å for iodide crystal-bar vanadium containing 150 ppm oxygen. The diffraction patterns of small chips of vanadium were photographed in a Debye-Scherrer camera with copper radiation. The lattice constant was calculated from the (321) reflection only.

B. Solubility Limits of Interstitials

Carbon is only slightly soluble in vanadium, according to Rostoker (39) and Rostoker and Yamamoto (41). Commercially pure vanadium containing as little as 360 ppm carbon has a second phase which Clough and Pavlovic (8) have identified as V_2C . This compound was studied by Schönberg (44) and found to have a hexagonal unit cell of interstitial A 3 type with $a = 2.881$ Å and $c = 4.547$ Å at 8% carbon. He found the solid solubility of carbon in vanadium to be as much as 2000 ppm at 1000°C.

The observations of Tammann and Schönert (50) that carbon does not readily diffuse into vanadium at 800°C to 900°C indicated a very low solubility. Furthermore, Powers and Doyle (36) have reported an instability of carbon solutions in vanadium from a decrease in the

carbon internal friction peak with time, caused by the precipitation of vanadium carbide from a supersaturated solution.

The solid solubility of nitrogen in vanadium has not been accurately determined. The work of Rostoker and Yamamoto (41) suggested a terminal solubility of less than 1%. They found a tetragonal phase at 5% nitrogen similar to the β phase in the V-O system. Clough and Pavlovic (8) found no evidence of a nitride phase in the microstructure of commercially pure vanadium containing 830 ppm nitrogen.

Hydrogen can be absorbed in large quantities by vanadium at high temperatures, with as much as 13 $\frac{w}{o}$ being retained at room temperature (23), and the hydrogen can be again removed by heating in a vacuum (39). Mallett and Bridge (30) have produced a hydride $VH_{0.94}$ having a tetragonal unit cell with the approximate parameters $a = 3.02 \text{ \AA}$ and $c = 3.36 \text{ \AA}$.

The solid solubility of oxygen in vanadium seems to increase from less than 0.25% to about 1.0% with increasing temperature (39). Rostoker and Yamamoto (42) have stated that the solubility is somewhere between 0.07% and 0.25% at temperatures below 900°C but that around 1850°C the maximum solubility is nearly 1%. This supports the work of Allen et al. (1) who calculated from their free energy determinations that the second phase (VO) appears at approximately 0.25% oxygen at 1000°C . However, the study of Seybolt and Sumsion (45) indicates considerably more solubility. From their precise lattice parameter measurements they found the solubility of oxygen at 600°C to be approximately 3.2 atomic per cent, which is 1.0 weight per cent. Furthermore, the solubility was not found to vary greatly with temperature. The β phase has been found

(42) to be body-centered tetragonal with $a = 3.01 \text{ \AA}$ and $c = 3.31 \text{ \AA}$ at 5% oxygen.

C. Hardness and Work Hardening

The effect of oxygen on the hardness of vanadium has been determined by Rostoker and Yamamoto (42) and by Seybolt and Sumsion (45) for oxygen concentrations from 0.1% to 5%. Their data are in fairly good agreement (39) and show a nearly linear relationship between Vickers Hardness Number and oxygen concentration up to 2% oxygen. No thorough study has been made of the hardness of vanadium containing smaller amounts of oxygen.

Nash et al. (33) found crystal-bar vanadium containing 120 ppm O, 80 ppm N, and 50 ppm H to have a hardness of 84 DPH. After cold-rolling and annealing, it had a hardness of 64 DPH. Removal of hydrogen by the anneal could account for this change.

A study by Beatty (4) indicates that nitrogen has nearly as great an effect on the hardness of vanadium as does oxygen. Baker and Ramsdell (2), however, found oxygen to influence the mechanical properties much more than nitrogen. Rostoker (39) has summarized some of the published values of hardness and purity of vanadium, the lowest hardness being 84 DPH.

Cold working hardens vanadium very slowly according to Rostoker et al. (40), who used calcium-reduced vanadium with an annealed hardness of approximately 175 DPH. Nash et al. (33) found that the hardness of iodide crystal-bar nearly doubles with cold work. The study by Baker

and Ramsdell (2) on electrolytic vanadium showed that most of the increase in hardness takes place within the first 5% reduction.

D. Embrittlement

Brown (5) first reported a brittle-ductile transition in vanadium, occurring between -80° and -30°C in an Izod impact test for vanadium containing 700 ppm oxygen, 700 ppm nitrogen, 40 ppm hydrogen, and 400 ppm carbon. An extensive investigation by Loomis and Carlson (27) of the brittle-ductile transition was made on two grades of vanadium in a study of the effect of both metallic and non-metallic impurities on the physical properties of vanadium. They observed a brittle-ductile transition temperature of -65°C to -10°C for calcium-reduced vanadium and -110°C to -10°C for iodide crystal-bar vanadium in tensile tests. A return of ductility was noted at lower temperatures.

Eustice and Carlson (16) found no embrittlement in vacuum-annealed iodide vanadium for temperatures down to -196°C . However, the presence of as little as 10 ppm hydrogen causes embrittlement over a narrow temperature range at approximately -100°C in tensile tests.

E. Tensile Properties

The tensile properties of vanadium have been investigated in a general way by several workers (33) (5) (42). Brown (5) observed an increase in strength from room temperature to 400°C in as-reduced vanadium, with the strength and ductility greatly dependent on the

interstitial impurities, especially oxygen and nitrogen. Lacy and Beck (25) reported a yield point of the order of 3000 to 5000 psi at room temperature and Pugh (37) found that it disappeared above 227°C.

A maximum in the tensile strength was observed by Rostoker et al. (43) near 300°C and by Brown (5) around 400°C for calcium-reduced vanadium. Pugh (37) (38) found maxima around 450°C in the tensile strength and the strain hardening exponent, and minima in the elongation and strain rate sensitivity at about the same temperature, for vanadium with 570 ppm oxygen, 90 ppm carbon, and 70 ppm nitrogen. A maximum in hardness for an annealing temperature of approximately 300°C has been observed by Baker and Ramsdell (2) with electrolytic vanadium. Nash et al. (33) found the strain hardening exponent of iodide vanadium to be 0.20 at room temperature but did not determine it as a function of temperature.

Eustice and Carlson (16) observed sharp serrations in the stress-strain curves between 140° and 180°C for high-oxygen vanadium.

Although the peaks in tensile strength, yield strength (38), and strain hardening exponent, and the serrated stress-strain curves indicate strain aging the impurity responsible has not been identified (39) (19).

F. Diffusion of Interstitials

The diffusion of oxygen in vanadium has been studied by Powers (35) who measured the shift in the oxygen internal friction peak temperature when the frequency of oscillation was varied. He found the oxygen peak at 186°C at 1 cps and calculated the activation energy for diffusion to

be 28,600 cal/g-atom. By the same method, Stanley and Wert (48) determined the diffusion coefficient of oxygen in vanadium to be $D_{O-V} = 0.003 \exp (-28,200/RT) \text{ cm}^2/\text{sec}$. Powers and Doyle (36) later separated the oxygen and carbon peaks to get more accurate measurements. At high oxygen concentrations the oxygen peak shifted to 162°C at 1 cps, and a diffusion coefficient of $D_{O-V} = 0.019 \exp (-29,300/RT) \text{ cm}^2/\text{sec}$ was calculated from it.

Tichelaar et al. (51) have used stress-relaxation measurements under pressure to obtain an activation energy for diffusion of oxygen in vanadium of 27,900[±]900 cal/g-atom, at 1 kg/cm² pressure and 98°C. This value is in reasonable agreement with the internal friction results determined over a much wider temperature range.

The diffusion of nitrogen has been measured by Powers (35) with the internal friction apparatus and found to be 34,100 cal/g-atom for the peak at 272°C. Stanley and Wert (48) found the diffusion coefficient to be $D_{N-V} = 0.018 \exp (-35,100/RT) \text{ cm}^2/\text{sec}$. The nitrogen internal friction peak was observed at 262°C at 1 cps by Powers and Doyle (36) who noted an instability in the peak with time, indicating nitride precipitation. By measurement of stress relaxation as a function of pressure Tichelaar et al. (51) obtained an activation energy of 36,700[±]2,100 cal/g-atom for nitrogen diffusion.

The diffusion of carbon has been studied with the internal friction technique by Powers and Doyle (36). At high carbon concentrations the carbon peak was observed at 162°C at 1 cps. The diffusion coefficient which they obtained was $D_{C-V} = 0.0047 \exp (-27,300/RT) \text{ cm}^2/\text{sec}$.

G. Current Theories of Strain Aging

The principal phenomenon of strain aging is the return of the yield point after interruption and resumption of a strength test. In the temperature range where strain aging occurs the mechanical properties are greatly affected: the yield strength, ultimate strength, and strain hardening are a maximum, the ductility and strain rate sensitivity are a minimum, and serrations are generally observed in the stress-strain curves (19). In addition, strain aging alters certain anelastic effects, the electrical resistance, and magnetism (13).

Cottrell (10) (12) has explained strain aging as the process in which solute atoms migrate to dislocations and temporarily lock them. The main points of the theory which Cottrell and his co-workers have developed are outlined below.

1. Movement of solute atoms to the dislocations

The interstitial solute atoms, aided by thermal fluctuations, have enough mobility to migrate to positions of lowest energy in the non-homogeneous stress field caused by the presence of a dislocation. They relieve the stress around the dislocation and at a position r , θ , relative to the dislocation, they have an interaction energy of

$$V = \Delta v \frac{G \lambda (1 + \nu)}{3\pi(1 - \nu)} \frac{\sin \theta}{r},$$

with a positive edge dislocation, where Δv is the volume change caused by introduction of the interstitial atom, G is the rigidity modulus of the metal, ν is Poisson's ratio, and λ is the slip distance in the dislocation. The position of lowest energy for an interstitial atom the size of oxygen is at $\theta = 3\pi/2$ and

$r (= r_0) \simeq 2 \times 10^{-8}$ cm, which is just below the extra half-plane of atoms of the dislocation.

The interaction energy of 0.5 eV assumed by Cottrell (10) for carbon and nitrogen in iron can be corrected to the interaction energy of oxygen in vanadium from the equation given above. Substitution of the appropriate values for vanadium gives an interaction energy of 0.34 eV between oxygen and an edge dislocation in vanadium.

Cottrell and Bilby (13) have calculated that the number of interstitial atoms which segregate to a dislocation in time t is $n(t) = \alpha n_0 (ADt/kT)^{2/3}$, where n_0 is the initial number of atoms in solution, α is a constant approximately equal to 3, and D is the diffusion coefficient of the interstitial atom. The assumption is made that the center of the dislocation line acts as a solute atom sink during the early stages of diffusion so that the solute atoms which have already diffused to the dislocation will not hinder the diffusion of other impurity atoms. At a later stage an equilibrium will be reached, with as many solute atoms diffusing away from the dislocation as moving to it, according to calculations by Bullough and Newman (6).

Nabarro (32) has calculated the tetragonal distortion of interstitial atoms in the body-centered cubic lattice to show that these atoms will interact with screw dislocations as well as with edge dislocations. Furthermore, in addition to the elastic interaction, an expression for an electrical interaction between solute atoms and dislocations has been derived by Cottrell et al. (14).

2. Formation of the condensed atmosphere

In the first stage of segregation of interstitial atoms around a dislocation, at sufficiently low temperatures and for times brief enough for the $t^{2/3}$ equation of Cottrell and Bilby to hold, there will be a single line of solute atoms lying along the dislocation line at the position of lowest energy. This condensed atmosphere never has all available sites filled because the entropy is greater if a few remain empty. As the temperature is increased, more sites remain empty and the locking of the dislocation is weakened (12).

3. Formation of the secondary atmosphere

Above a certain critical temperature range the atoms become less concentrated and form a dilute atmosphere, or Maxwellian distribution, around the dislocation where the concentration of solute atoms with a binding energy V is $c = c_0 \exp (-V/kT)$, the over-all concentration of the solute atoms being c_0 . The critical temperature at which the secondary atmosphere begins to form is $T_0 = V_{\max}/k \log_e (1/c_0)$. Accordingly, Mott (31) has suggested that the temperature at which the yield point is no longer observed should be identified with T_0 , since a condensed atmosphere is needed for a strong yield point.

4. The yield point

Cottrell believes the yield point to be due to the strong interaction between dislocations and their atmospheres, so that the force required to pull the dislocations free will be greater than that

necessary to keep them in motion after they have escaped from their atmospheres. In this case the stress required to initiate yielding drops sharply at the beginning of plastic deformation, producing a yield point.

The stress required to pull a dislocation away from a condensed atmosphere is $\sigma_0 \approx A/b^2 r_0^2$ in which b is the magnitude of the burger's vector. The stress needed to pull a dislocation free of a dilute atmosphere is much smaller, according to Cottrell and Jaswon (15), and is approximately $\sigma_0 \approx 17 A c_0 N/b$, where N is the total number of atoms in a unit volume of the crystal. However, because the condensed atmosphere is highly localized, after a small length of dislocation is freed by thermal fluctuations the applied stress can pull away the rest of the dislocation. Once freed, it helps other dislocations to break away and causes yielding to develop catastrophically.

5. Strain aging

A sample strained beyond its yield point will not show another yield point if immediately reloaded, but an intermediate aging treatment will return the yield point, if the aging temperature is high enough to allow diffusion of solute atoms to relock the dislocations.

If the temperature of a tensile test is sufficiently high, interstitial atoms migrate during the test to form condensed atmospheres at dislocations. The release of the interaction energy occurs at the expense of dislocation kinetic energy, slowing down the dislocations. To continue plastic flow the stress must then be increased, which in-

creases the dislocation velocity and reduces atomic migration. These alternating speeds of the dislocations appear as serrations in the tensile stress-strain curve. Cottrell (11) has noted that the serration range for iron containing nitrogen occurs when the diffusion coefficient and the strain rate $\dot{\epsilon}$ are related by $D = 10^{-9} \dot{\epsilon}$. Using this equation, the temperature at which oxygen should cause strain aging in vanadium is found to be 310°C . Adjustment of the equation for an oxygen concentration of 150 ppm and the difference in interaction energy, by the method of Cottrell (11), gives a strain aging temperature of 290°C .

Harper (18) studied the strain aging of iron containing carbon by internal friction methods. His results show that segregation of carbon does vary with $t^{2/3}$, as Cottrell and Bilby (13) predicted, and from the variation with temperature he found the activation energy for strain aging to be the same as for the diffusion of carbon in iron.

III. MATERIALS

In a study of the effect of oxygen on the properties of a metal, the contamination by atmospheric oxygen is a major factor. Consequently, the analyses given in this work were determined after sample preparation and annealing on the actual samples that were tested.

A. Vanadium Metal

All of the vanadium used in this study was purified by the iodide crystal-bar process. A detailed description of the equipment and purification method has recently been published by Carlson and Owen (7). A typical analysis of the vanadium is given in Table 1.

Table 1. Typical analysis of vacuum-annealed crystal-bar vanadium

Element	Weight, %	Element	Weight, %
O	0.010	Si	< 0.005
N	< 0.0005	Cu	0.003
H	0.0001	Ni	0.002
C	0.015	Ca	< 0.002
Fe	0.015	Mg	< 0.002
Cr	0.007	Ti	< 0.002
Not detected: Al, Ag, As, Au, B, Be, Bi, Cd, Ge, Hf, Hg, Mn, Mo, Na, Nb, P, Pb, Pt, Sb, Sn, Ta, Te, Tl, W, Zn, Zr			

The oxygen, nitrogen, and hydrogen in the vanadium samples were measured by vacuum fusion methods and the nitrogen was also analyzed by the micro-Kjeldahl method. Carbon was determined in an inert gas fusion apparatus. The metallic impurities in vanadium were analyzed spectrographically.

The vanadium of higher oxygen content was prepared by arc-melting crystal-bar vanadium with an oxygen master alloy in a reduced atmosphere of helium. The metal was then swaged to a 1/4 inch diameter rod, cut into short sections, and again arc-melted several times to achieve uniformity of oxygen throughout the sample. The master alloys containing 0.7 % oxygen were prepared from a crystal-bar vanadium button into which holes were drilled. The holes were filled with purified V_2O_5 and plugged, and the button was then arc-melted slowly to minimize volatilization of V_2O_5 .

In order to obtain vanadium containing less than 50 ppm oxygen, crystal-bar vanadium was given an additional treatment with calcium. Pieces of crystal-bar vanadium were placed in a tantalum crucible with high-purity calcium metal, the crucible was welded shut in a helium atmosphere and placed in an inconel container which also was welded shut in helium. The vanadium and calcium were then heated at 1100°C for four days to reach an equilibrium between the oxygen in solid solution in the vanadium and calcium oxide. After the run the calcium and calcium oxide were removed from the vanadium metal by pickling with dilute acetic acid. By this method the oxygen concentration of vanadium has

been reduced to approximately 15 ppm in experiments by Peterson.¹

B. Sample Preparation

X-ray samples for lattice constant determination were prepared by cold rolling vanadium to a thickness of 0.01 inch. A sample was cut from this sheet and bent to a curve of 60 mm radius to fit the back-reflection focusing camera. The metal was annealed in a dynamic vacuum of 10^{-7} mm Hg for four hours at 900°C to remove hydrogen from the metal and to recrystallize it into a fine-grained structure.

Bend test specimens were prepared by rolling arc-melted vanadium into plates of 0.070 inch thickness. Samples containing more than 0.3% oxygen were jacketed in mild steel in a helium atmosphere and hot-rolled at 700°C . From this metal samples were cut and milled to specimens 0.250 inch in width and approximately 1 1/2 inches long. They were ground to a thickness of 0.060 inch on a kerosene-cooled belt grinder, polished on 600 grit paper, and electropolished with a saturated oxalic acid electrolyte. They were then annealed in a vacuum of 10^{-7} mm for four hours at 900°C .

Tensile test specimens were prepared from vanadium by swaging to 3/16 inch diameter rod and turning on a lathe to the dimensions given in Figure 1. Threading was done with die and sample aligned in the lathe. All machining and threading were carried out under a stream of coolant, producing a mirror-like finish on the tensile specimens. The final annealing treatment was at 900°C for four hours in a dynamic vacuum of 10^{-7} mm.

¹Peterson, David T. Iowa State University, Ames, Iowa. Private communication. 1961.

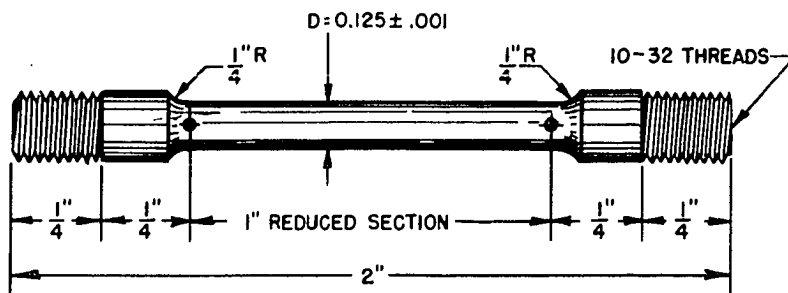


Figure 1. Tensile test specimen

IV. APPARATUS AND EXPERIMENTAL METHODS

The apparatus and methods were selected from the standpoints of 1) accuracy, 2) appropriateness for the material and the experiment, and 3) comparison with previous work in the field.

A. Lattice Constant Determination

The lattice constant measurements were made on polycrystalline sheet samples prepared as previously described, with a back-reflection focusing camera of 60 mm radius. Molybdenum x-radiation was used with a zirconium filter to remove the $K\beta$ lines. The exposure was made in an atmosphere of helium with mechanical oscillation of the sample. Seventeen $K\alpha$ lines, the reflections from (552) to (822), were visible and all were used in the initial calculations. By the use of Cohen's least-squares method (9) the lattice constants were calculated as functions of $(\frac{\pi}{2} - \theta) \cot \theta$ and mathematically extrapolated to $\theta = \frac{\pi}{2}$, where θ is the diffraction angle, to determine the best value of the lattice constant for that sample.

Because of the recent criticism (49) of Cohen's method the lattice constants were recalculated from the $K\alpha_1$ (644) and (820) reflections at $\theta = 75^\circ$, the (653) reflection at $\theta = 78^\circ$, and the (822) and (660) reflections at $\theta = 83^\circ$ for comparison with the Cohen method. The distances between the lines were measured to the nearest 0.05 mm with a film shrinkage correction made from camera fiducial marks. The lattice constants obtained from the three lines were consistent to within

$\pm 0.0002 \text{ \AA}$ and essentially independent of the angle of diffraction, and therefore were averaged to get the best value of the lattice constant with a probable error of $\pm 0.0001 \text{ \AA}$.

B. Hardness Measurements

Hardness values were determined on a Kentron microhardness tester with a diamond pyramid indenter. Hardness values reported in this study are all DPH (Diamond Pyramid Hardness, Vickers Hardness Number) which are identical to Brinell hardness for all the alloys in these experiments.

C. Bend Test Apparatus

The low-temperature bend test apparatus, as shown in Figure 2, consisted essentially of two hardened steel rollers $25/32$ inch apart, upon which the test specimen rested, and a steel knife-edge which pressed down upon the center of the specimen. A copper-constantan thermocouple was pressed against the sample so that contact was maintained throughout the bend test. Temperatures as low as -180°C were maintained in the test chamber by introduction of nitrogen vapor from a liquid nitrogen tank. A Brown temperature controller alternately operated solenoid valves, forcing cold nitrogen or warm helium into the bend test chamber. Temperatures down to -100°C were maintained to within $\pm 1^{\circ}\text{C}$. The deviation of temperatures from -100° to -180°C was $\pm 2^{\circ}\text{C}$. Bend tests at -196°C were made with the addition to the apparatus of a

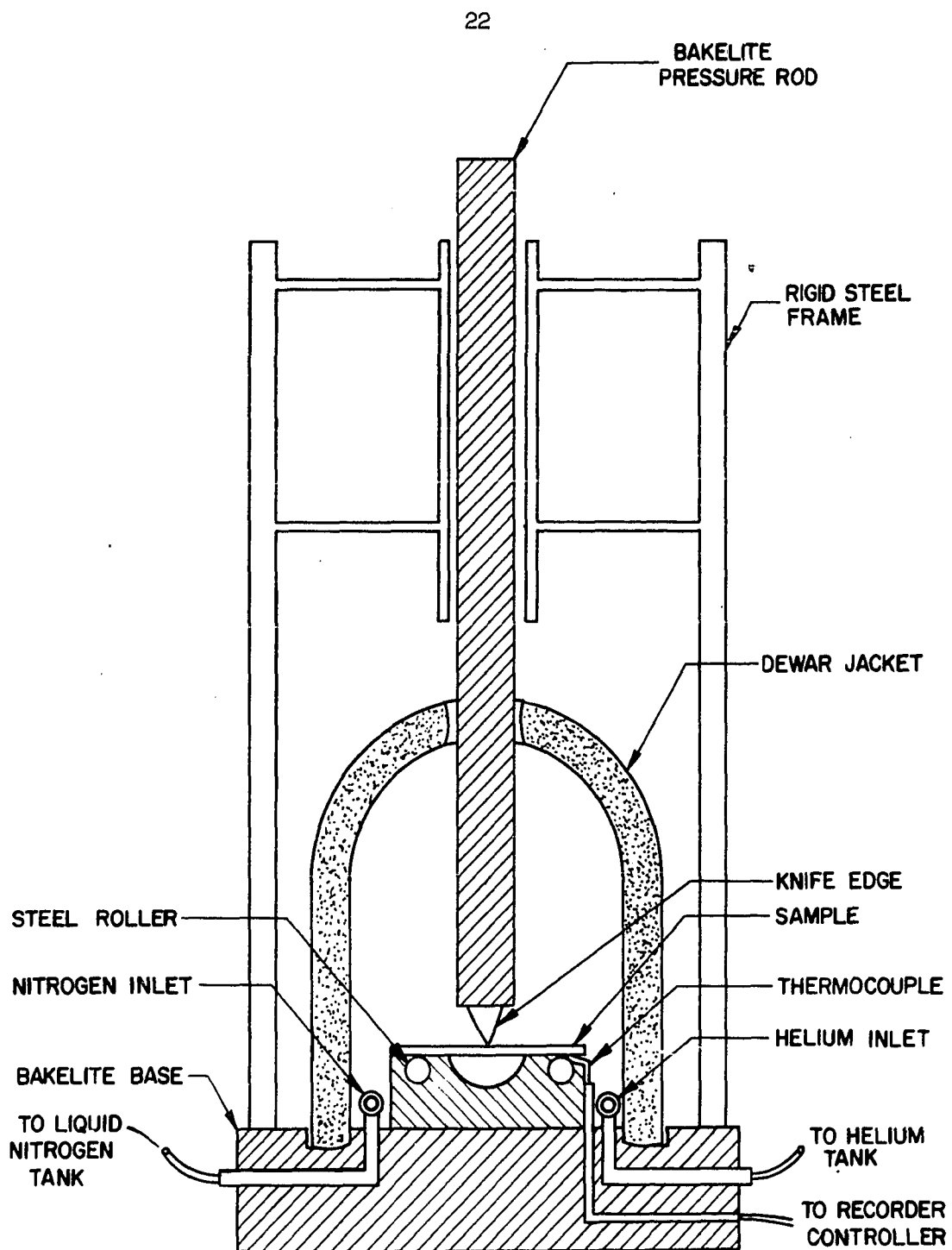


Figure 2. Low-temperature bend test apparatus

stainless steel cup which was filled with liquid nitrogen, immersing sample, mount, and knife-edge.

The pressure rod was forced downward on the specimen at a constant speed of 0.01 inch per minute by means of a Tinius-Olsen testing machine equipped with an X-Y recorder. The bending load on the sample was recorded as a function of the displacement of the pressure rod.

D. Tensile Test Apparatus

Tensile tests from room temperature to 500°C were performed on a screw-driven Tinius-Olsen tensile testing machine equipped with an X-Y recorder and an external extensometer to record crosshead motion. The high-temperature tensile tests were conducted in an atmosphere of helium to prevent atmospheric contamination. A diagram of the test chamber is shown in Figure 3. The furnace temperature was maintained with a Brown controller which held the temperature of the sample to within $\pm 0.5^\circ\text{C}$ during the test.

Crosshead speed of the testing machine was 0.01 inch per minute for all tensile tests except for momentary changes to 0.10 inch per minute on some tests to determine strain rate sensitivity.

Aging experiments to determine the activation energy for yield point return were made on room-temperature tensile tests by unloading the sample, heating it for a time long enough to permit return of the yield point, and then resuming the tensile test. For short aging times the sample was heated in an oil bath to speed temperature equilibrium, while long aging was conducted in a resistance furnace.

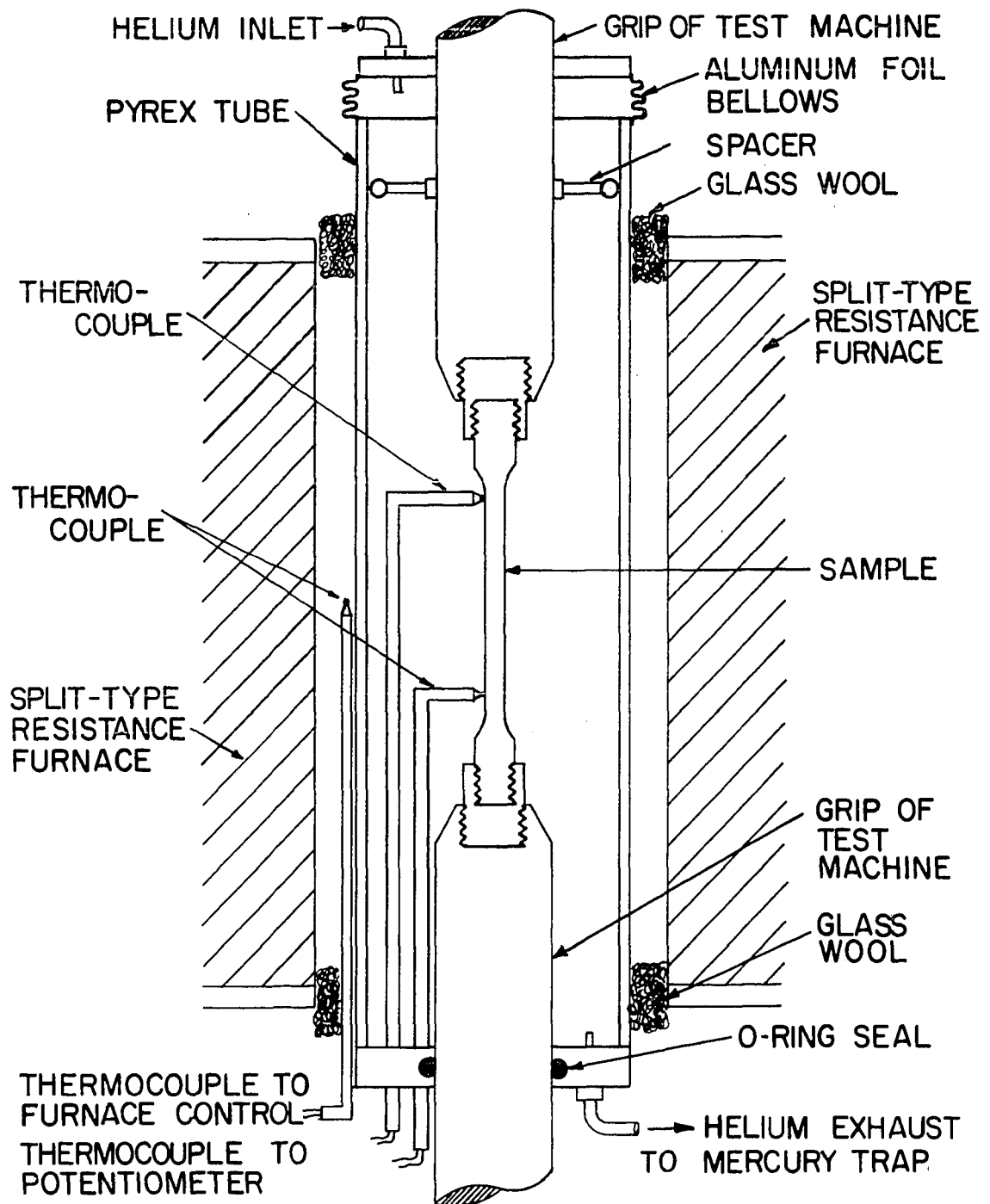


Figure 3. Tensile test chamber

V. PRESENTATION AND INTERPRETATION OF EXPERIMENTAL RESULTS

In addition to a statement of the results of the experiments, it has been found necessary for clarity in some instances to include a comparison with previous work in the field and a derivation of the theoretical basis of the experiment.

A. Lattice Constant Results

The lattice constant of vanadium has been determined as a function of oxygen content. Oxygen present in solid solution expands the vanadium lattice, increasing the lattice constant by approximately 1.5×10^{-6} Å/ppm. This is shown in the graph (Figure 4) which was taken from the data in Table 2 calculated from the high-angle $K\alpha_1$ reflections.

Table 2. Lattice constant of vanadium
at various oxygen concentrations

Lattice constant, Ångstroms	Oxygen content, ppm
3.0258 Å	47 ppm
3.0259	65
3.0265	150
3.0264	220
3.0265	315
3.0269	608
3.0267	610
3.0272	830
3.0275	1100
3.0281	1410
3.0291	2140
3.0303	2880
3.0304	2970

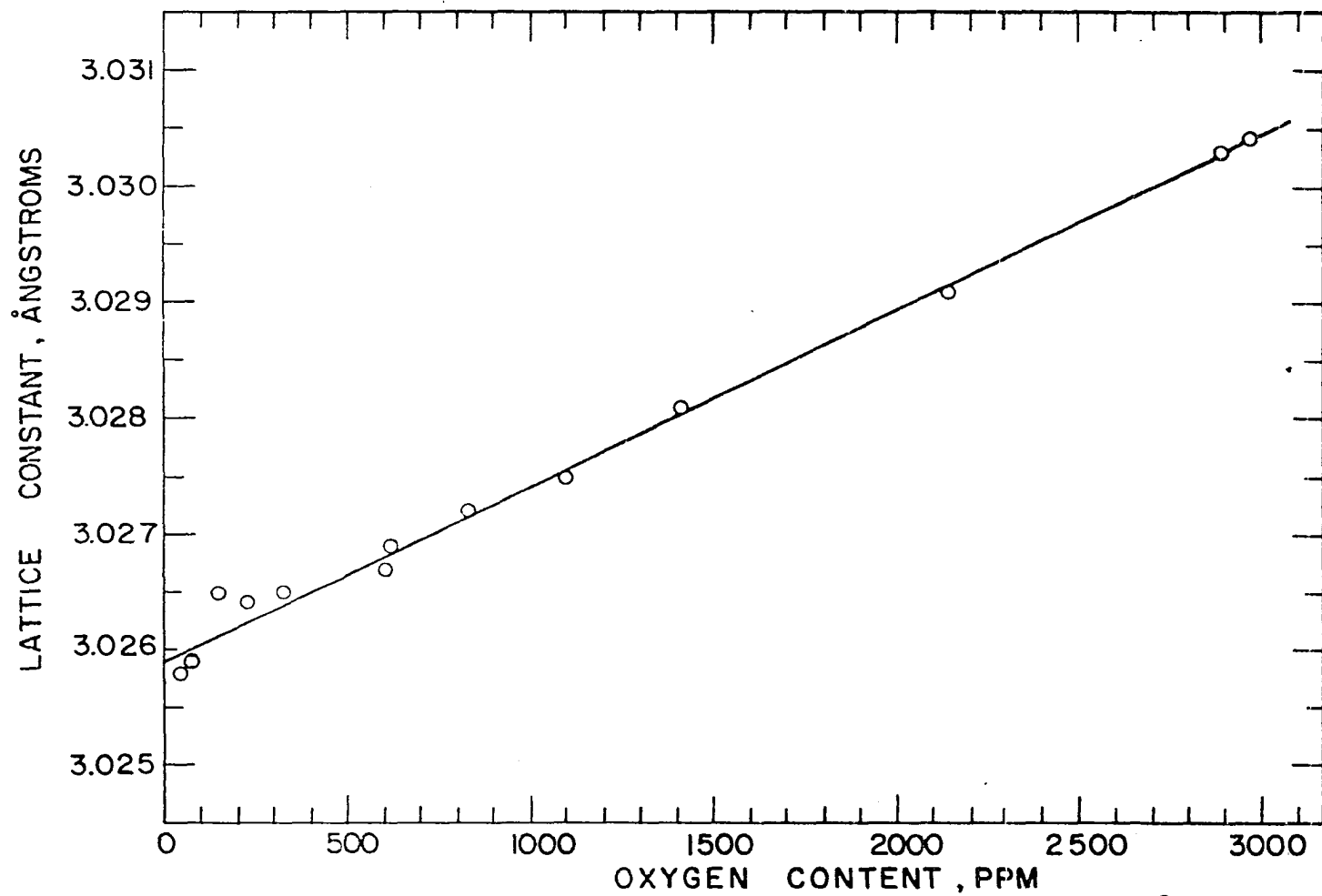


Figure 4. Effect of oxygen on the lattice constant of vanadium at 25°C

The lattice constant of oxygen-free vanadium at 25°C, as determined by extrapolation in Figure 4, is 3.0259 ± 0.0002 Å. Variation of carbon content in the range of 100 ppm to 450 ppm was observed to have virtually no effect on the lattice constant. However, hydrogen has a pronounced effect on the lattice. Leaching a vanadium sample in dilute HCl increased the lattice constant from 3.0264 Å to 3.0308 Å. An annealing treatment of one hour at 600°C in high vacuum to remove the hydrogen lowered the lattice constant to its original value.

From the vanadium lattice constant of 3.0259 Å the effective atomic radius was calculated to be 1.3102 Å and the x-ray density to be 6.107 ± 0.001 grams/cm³ at 25°C. All of the samples used for x-ray lattice constant determination were annealed at 900°C for four hours. It can be inferred from the regular increase in the lattice constant with increasing oxygen content that oxygen solubility in vanadium is in excess of 0.30 w/o at 900°C. Inasmuch as the samples were furnace cooled, it is probable that the ambient solubility of oxygen is greater than 0.30 w/o.

B. Hardness, Work Hardening, and Microstructure

The hardness of vanadium was observed to be sensitive to the amount of oxygen dissolved in the metal. In fact, the hardness can be used as a measure of the oxygen content, as is shown by Figure 5, the relationship between oxygen content and Diamond Pyramid Hardness. The hardness values were determined on fully annealed vanadium. This curve connects smoothly with the data of Seybolt and Sumsion (45) who determined the effect of oxygen at higher concentrations.

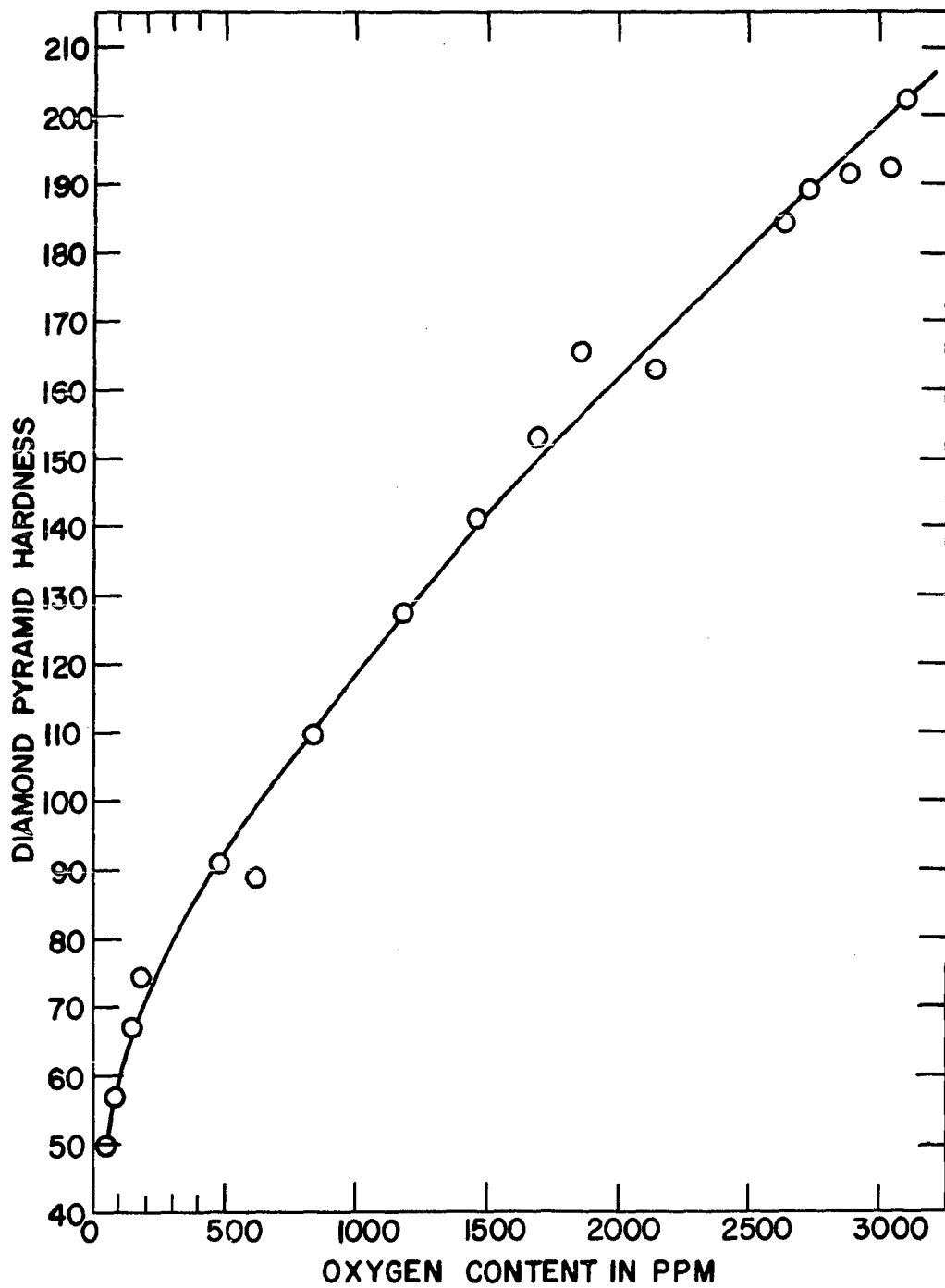


Figure 5. Effect of oxygen on the hardness of vanadium

A sample of crystal-bar vanadium which had been given a calcium treatment to remove oxygen was cold rolled to study the work hardening of the metal. The hardness increased rapidly with the first 3% of cold reduction but further working increased the hardness only slightly. The results of the work hardening experiment are shown in Figure 6. For comparison, the data of Rostoker et al. (40) on calcium-reduced vanadium, Baker and Ramsdell (2) on electrolytic vanadium, and Nash et al. (33) on crystal-bar vanadium are also included.

The microstructures of vanadium samples containing up to 3100 ppm oxygen and annealed at 900°C showed no evidence of a second phase, thus indicating the solubility of oxygen in vanadium to be greater than 0.3% at 900°C.

C. Results of Bend Tests

Bend tests were performed on vanadium samples containing from 150 ppm to 3100 ppm oxygen, at temperatures from 22°C to -196°C. The results of these tests are tabulated in Tables 3 through 16. The low-oxygen samples exhibited a yield point, but for samples that did not, the yield load was measured at 0.002 inch deflection (approximately equivalent to 0.2% offset for tensile tests). Both the yield load and load at maximum strength have a region of proportionality with the reciprocal of the absolute temperature which is shown in Figures 7 and 8. The yield load becomes invariant with temperature below -160°C, although the maximum bending load remains proportional to $1/T$ down to approximately -180°C. The slopes of the straight-line portion of the curves increase

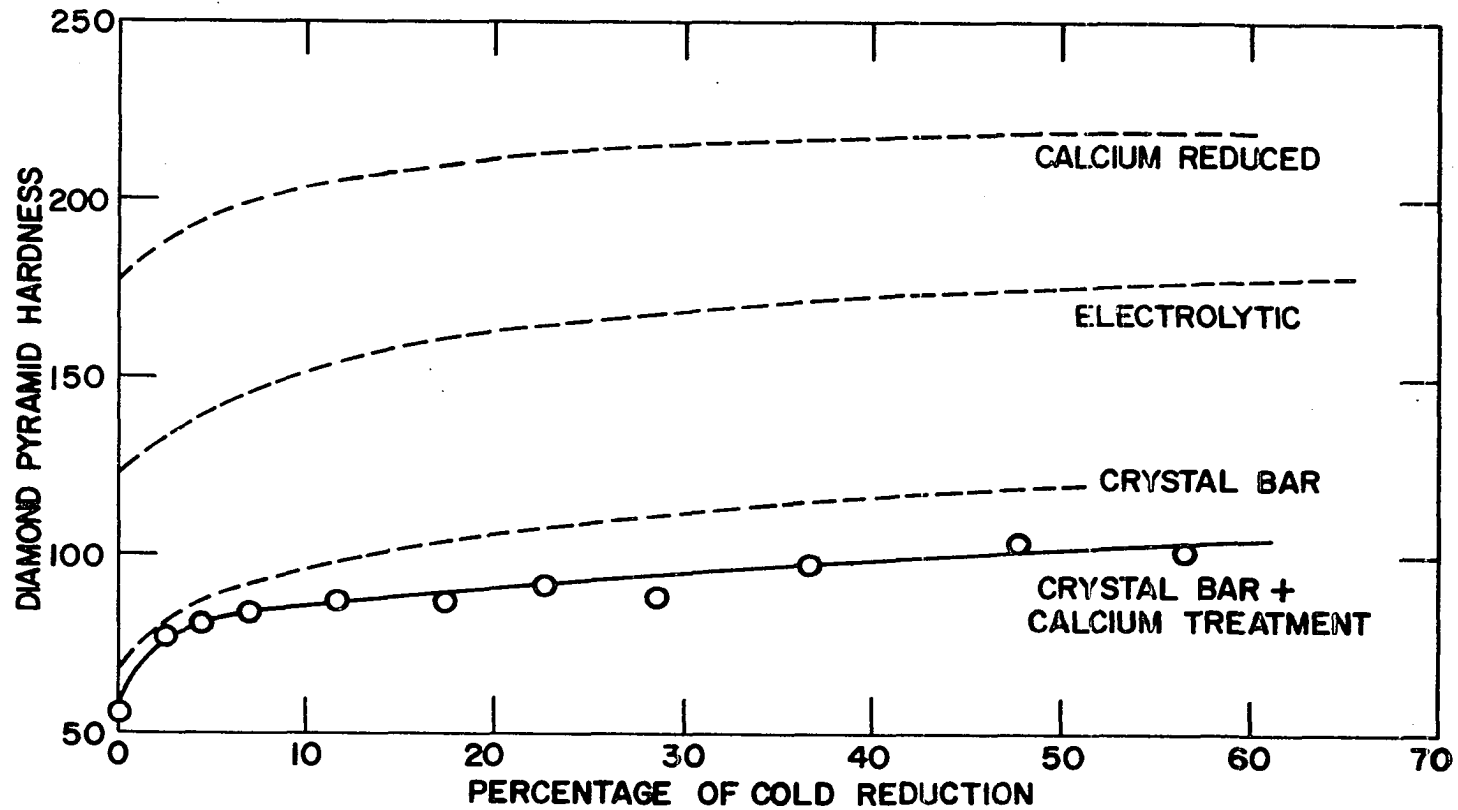


Figure 6. Work hardening of vanadium

Table 3. Bend tests of vanadium containing 150 ppm oxygen

Test temperature	Maximum bending load	Yield load	Total deflection	Type of bend
22°C	2,770 psi	1,200 psi	0.300 in.	Ductile
0	3,000	1,340	"	"
- 50	3,180	1,820	"	"
-100	4,640	3,030	"	"
-120	5,550	4,350	"	"
-130	5,580	4,470	"	"
-150	6,690	6,200	"	"
-170	8,470	7,000	"	"
-196	10,010	7,280	"	"

Table 4. Bend tests of vanadium containing 490 ppm oxygen

Test temperature	Maximum bending load	Total deflection	Type of bend
22°C	4,190 psi	0.300 in.	Ductile
0	3,990	"	"
- 50	4,970	"	"
-100	5,840	"	"
-120	7,650	"	"
-130	6,690	"	"
-150	7,700	"	"
-170	10,250	"	"
-196	12,130	"	"

Table 5. Bend tests of vanadium containing 700 ppm oxygen

Test temperature	Maximum bending load	Total deflection	Type of bend
22°C	5,130 psi	0.300 in.	Ductile
0	4,680	"	"
- 50	5,650	"	"
-100	6,790	"	"
-120	8,520	"	"
-130	8,160	"	"
-150	9,070	"	"
-170	9,950	"	"
-180	10,810	"	"
-196	11,860	"	"

Table 6. Bend tests of vanadium containing 840 ppm oxygen

Test temperature	Maximum bending load	Yield load	Total deflection	Type of bend
22°C	5,050 psi	2,940 psi	0.300 in.	Ductile
- 50	6,420	---	"	"
-100	7,920	5,590	"	"
-120	9,650	7,010	"	"
-130	9,180	7,260	"	"
-150	10,310	8,940	"	"
-170	12,400	10,400	"	"
-196	13,980	10,300	"	"

Table 7. Bend tests of vanadium containing 1050 ppm oxygen

Test temperature	Maximum bending load	Total deflection	Type of bend
22°C	6,600 psi	0.300 in.	Ductile
0	6,520	"	"
- 50	7,460	"	"
-100	8,350	"	"
-120	9,670	"	"
-130	10,800	"	"
-150	12,150	"	"
-170	11,090	"	Crack
-180	14,840	"	Ductile
-196	14,220	"	"

Table 8. Bend tests of vanadium containing 1180 ppm oxygen

Test temperature	Maximum bending load	Total deflection	Type of bend
22°C	6,260 psi	0.300 in.	Ductile
0	6,190	"	"
- 50	7,000	"	"
-100	9,460	"	"
-120	10,840	"	"
-130	11,290	"	"
-150	10,790	"	Edge cracks
-170	(12,290)	0.073	Brittle
-196	15,360	0.300	Ductile

Table 9. Bend tests of vanadium containing 1300 ppm oxygen

Test temperature	Maximum bending load	Total deflection	Type of bend
22°C	7,270 psi	0.300 in.	Ductile
0	7,660	"	"
- 50	7,960	"	"
-100	9,580	"	"
-120	11,120	"	"
-130	12,060	"	"
-150	13,470	"	"
-170	(11,510)	0.024	Brittle
-180	15,420	0.222	Crack
-196	15,610	0.300	Ductile

Table 10. Bend tests of vanadium containing 1320 ppm oxygen

Test temperature	Maximum bending load	Yield load	Total deflection	Type of bend
22°C	7,260 psi	4,290 psi	0.300 in.	Ductile
0	7,330	4,650	"	"
- 50	8,100	6,100	"	"
-100	10,910	7,770	"	"
-120	11,490	9,210	"	"
-130	12,640	9,700	"	"
-150	12,340	11,080	"	Edge crack
-170	15,260	12,300	"	Ductile
-196	17,320	12,210	0.255	Crack

Table 11. Bend tests of vanadium containing 1420 ppm oxygen

Test temperature	Maximum bending load	Total deflection	Type of bend
22°C	7,470 psi	0.300 in.	Ductile
0	8,100	"	"
- 50	8,590	"	"
-100	11,150	"	"
-120	11,490	"	"
-130	12,790	"	"
-150	14,220	"	"
-170	13,670	"	"
-180	14,650	"	"
-196	15,400	"	"

Table 12. Bend tests of vanadium containing 1605 ppm oxygen

Test temperature	Maximum bending load	Total deflection	Type of bend
22°C	8,100 psi	0.300 in.	Ductile
0	7,710	"	"
- 50	9,080	"	"
-100	11,630	"	"
-120	12,480	"	"
-130	13,520	"	"
-150	14,000	"	"
-170	16,200	"	"
-180	17,070	"	"
-196	(15,390)	0.052	Brittle

Table 13. Bend tests of vanadium containing 1690 ppm oxygen

Test temperature	Maximum bending load	Yield load	Total deflection	Type of bend
24°C	7,250 psi	4,390 psi	0.300 in.	Ductile
0	7,730	5,160	"	"
- 50	8,680	6,250	"	"
-100	11,720	8,640	"	"
-120	12,170	9,230	"	"
-130	12,410	10,450	"	"
-140	12,670	10,730	"	"
-150	(12,300)	(11,280)	0.028	Brittle
-170	(14,700)	(12,340)	0.121	"
-196	(14,320)	(11,000)	0.132	"

Table 14. Bend tests of vanadium containing 1705 ppm oxygen

Test temperature	Maximum bending load	Yield load	Total deflection	Type of bend
22°C	7,610 psi	4,610 psi	0.300 in.	Ductile
0	8,330	5,490	"	"
- 50	8,120	6,100	"	"
-100	11,080	8,210	"	"
-120	13,190	10,380	"	"
-125	13,400	10,500	"	"
-130	(10,150)	(9,400)	0.223	Brittle
-150	(11,690)	(11,400)	0.033	"
-170	(13,780)	(12,160)	0.046	"
-196	(6,740)	(5,900)	0.029	"

Table 15. Bend tests of vanadium containing 1850 ppm oxygen

Test temperature	Maximum bending load	Yield load	Total deflection	Type of bend
22°C	8,190 psi	5,230 psi	0.300 in.	Ductile
0	9,490	6,320	"	"
- 50	9,840	7,150	"	"
-100	12,160	8,960	"	"
-120	13,230	10,480	"	"
-125	13,450	11,440	"	"
-130	(12,800)	(12,150)	0.105	Brittle
-135	(11,150)	(11,140)	0.017	"
-150	(10,590)	(10,050)	0.047	"
-170	(7,410)	(7,400)	0.015	"
-196	(7,710)	(7,130)	0.021	"

Table 16. Bend tests of vanadium containing over 2500 ppm oxygen

Oxygen content	Test temperature	Maximum bending load	Total deflection	Type of bend
2625 ppm	- 80°C	11,450 psi	0.300 in.	Ductile
"	- 85	(5,000)	0.015	Brittle
"	- 95	(10,450)	0.036	"
2730 ppm	- 70°C	12,450 psi	0.300 in.	Ductile
"	- 75	11,300	0.300	"
"	- 77	(6,900)	0.019	Brittle
"	- 80	(9,400)	0.030	"
"	- 85	(11,000)	0.086	"
2740 ppm	- 50°C	10,500 psi	0.300 in.	Ductile
"	- 85	(8,800)	0.028	Brittle
"	-196	(11,600)	0.023	"
3040 ppm	- 50°C	13,900 psi	0.300 in.	Ductile
"	- 65	9,800	0.171	Crack
"	- 68	10,750	0.300	Ductile
"	- 72	14,050	0.300	"
"	- 75	(9,850)	0.031	Brittle
"	- 80	(10,600)	0.035	"
"	-100	(11,300)	0.030	"
3100 ppm	- 45°C	(11,000 psi)	0.062 in.	Brittle
"	- 55	(9,200)	0.036	"
"	- 60	(10,050)	0.078	"
"	- 70	(9,350)	0.026	"

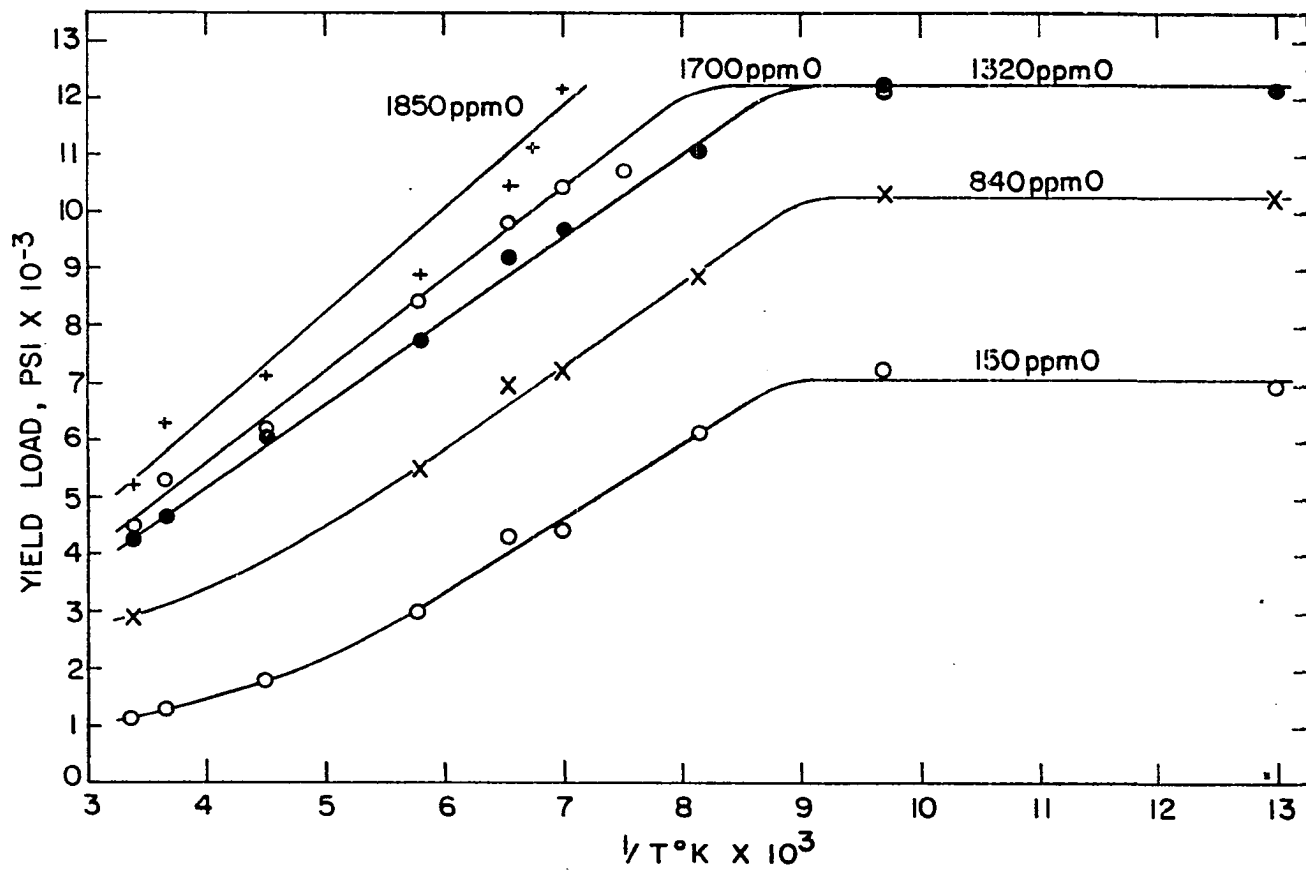


Figure 7. Effect of temperature and oxygen on the yield load in bend tests

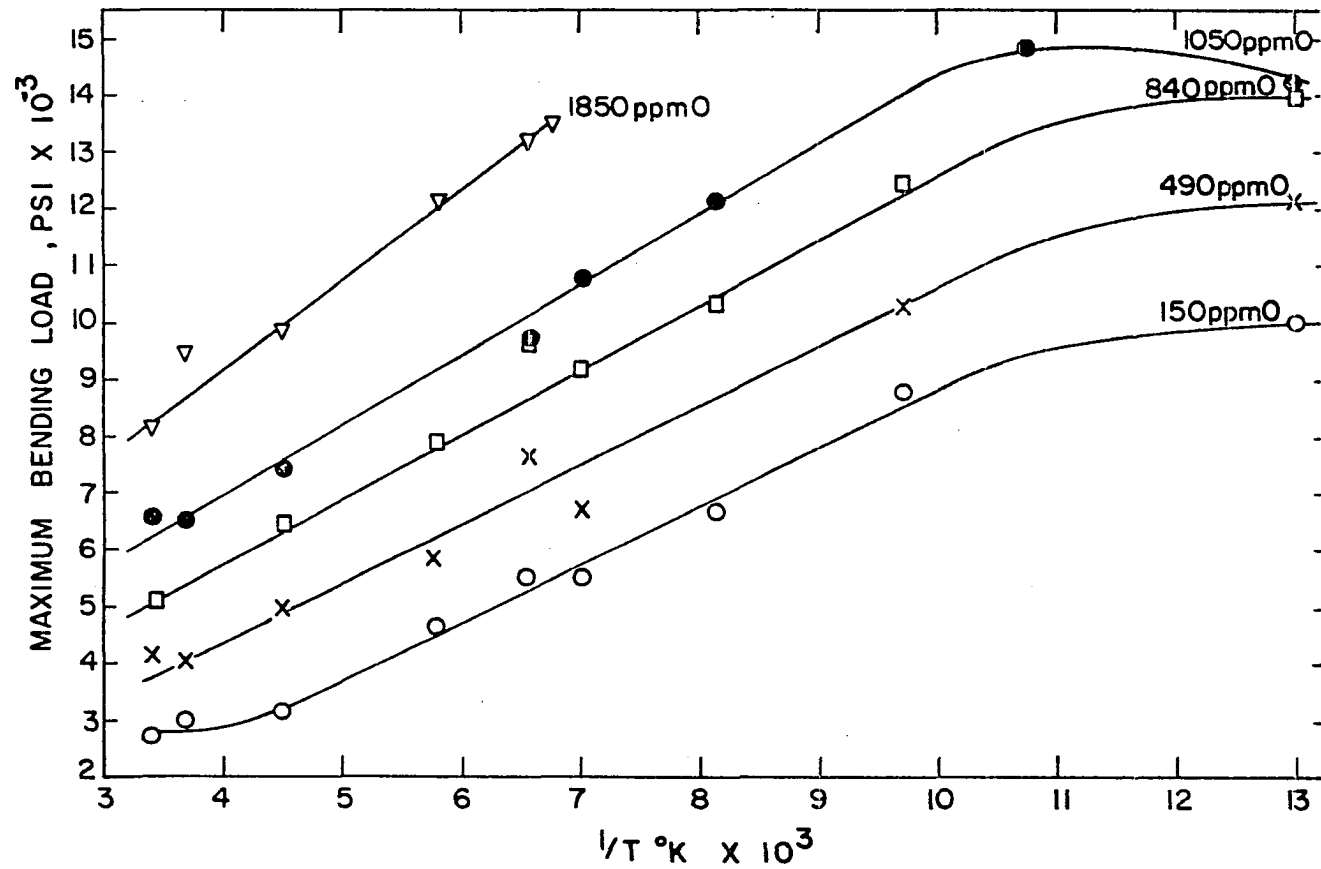


Figure 8. Effect of temperature and oxygen on the maximum bending load

slightly with increasing oxygen concentration for both yield load and maximum load. It should be noted that all bend samples from 1320 ppm to 1850 ppm oxygen had the same yield load at low temperatures where the yield load is not a function of temperature.

The yield loads and maximum bending loads given in Tables 3 through 16 and plotted in Figures 7 and 8 were calculated by dividing the total load on the specimen by its cross-sectional area. The geometry of the apparatus, of course, has a great effect on the load. The mechanical advantage of the bend test apparatus, which varies somewhat with strain, was calculated to be approximately 12.5 at maximum load, assuming that the bend test specimen deforms in tension in a circular arc around the point of application of the load. This assumption is particularly poor for high-oxygen samples that bend with a large radius of curvature, so that the actual values of the mechanical advantage found by comparison of tensile and bend tests vary from 7 to 9. Therefore, bend test loads in this apparatus must be multiplied by a factor of 8 to approximate their equivalent tensile stresses.

Bend tests were classified as ductile if the sample bent to a 90° angle without cracking, with a deflection of 0.300 inch from the original position, and were called brittle if they cracked before a deflection of 0.300 inch was reached. In almost every case, brittle samples fractured under very small deflections, so that the temperature of median deflection was chosen as the brittle-ductile transition temperature of the sample. The effect that oxygen has on the brittle-ductile transition temperature of vanadium is shown in Figure 9 which was plotted from the

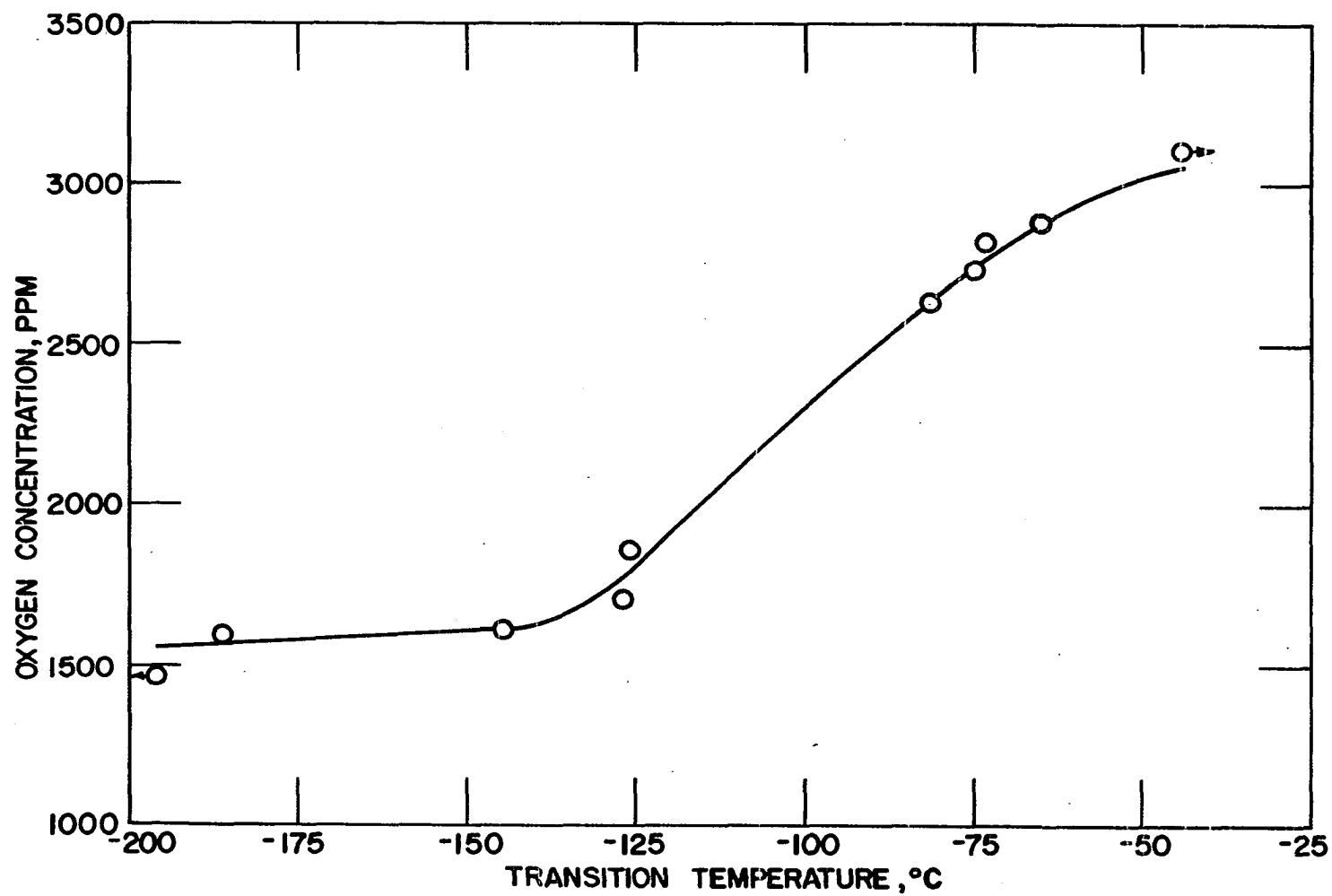


Figure 9. Effect of oxygen on the brittle-ductile transition of vanadium

data in Table 17. No embrittlement down to -196°C was observed for samples containing less than 1500 ppm oxygen, but for higher concentrations the transition temperature was greatly affected by the amount of oxygen present. No return of ductility at low temperatures, such as has been reported for hydrogen embrittlement of vanadium (16), was found for oxygen embrittlement.

Table 17. Brittle-ductile transition temperatures of vanadium from bend tests

Oxygen content	Transition temperature
≤ 1460 ppm	$< -196^{\circ}\text{C}$
1605 ppm	-187°C
1690 ppm	-145°C
1705 ppm	-127°C
1850 ppm	-126°C
2625 ppm	-82°C
2730 ppm	-75°C
2740 ppm	-65°C
3040 ppm	-73°C
3100 ppm	$> -44^{\circ}\text{C}$

D. Results of Tensile Tests

Summaries of some of the important tensile properties found for vanadium containing from 47 to 1800 ppm oxygen at temperatures from

room temperature to 500°C are given in Tables 18 through 22. The effect of oxygen on tensile properties of vanadium at room temperature is illustrated in Figure 10, which is a graph of the upper yield point and proportional limit, the lower yield point, the ultimate tensile strength, and the true stress at maximum load. All of these factors are similarly affected by oxygen in the metal, being nearly linear above 200 ppm oxygen. The true stress at maximum load is related to the tensile strength by the equation $\sigma = S(1 + \epsilon)$, where σ is the true stress, S is the tensile strength, and ϵ is the uniform elongation.

A proportional relationship was found between the Diamond Pyramid Hardness and the stress at maximum load at room temperature, as shown in Figure 11. The hardness values of the tensile samples were obtained from the graph of hardness versus oxygen content (Figure 5). This relationship holds for vanadium in which only the oxygen content is varied. For example, the tensile tests of Brown (5), with conversion of his Rockwell B hardness values to DPH by means of the graph of Rostoker (39), show considerable scatter from the straight-line relationship in Figure 11 probably because of the wide variation in the other interstitial impurities.

Other room temperature tensile properties determined were the percent uniform elongation and the strain hardening exponent n , defined by the equation $\sigma = \sigma_0 \epsilon^n$ where σ is the true stress, σ_0 is the stress at unit strain, and ϵ is the true strain. The rapid increase in these properties as the oxygen content decreases is shown in Figure 12. The anomalous maximum in the uniform elongation at low oxygen contents may

Table 18. Tensile properties of vanadium containing 47 ppm oxygen

Test temperature	Tensile strength	Yield strength	Uniform elongation	Strain hardening exponent
23°C	18,950 psi	5,200 psi	18.5%	0.499
98	17,300	4,000	19.5	0.479
150	15,600	---	---	---
175	15,750	3,300	22.1	0.483
200	16,300	3,400	17.0	0.456
250	18,000	5,150	18.5	0.414
300	26,400	5,350	16.9	0.529
350	27,800	6,600	15.0	0.541
375	28,200	6,100	16.5	0.564
400	27,100	6,250	20.5	0.526
450	25,900	5,000	17.9	0.513
500	21,100	3,300	16.3	0.503

Table 19. Tensile properties of vanadium containing 150 ppm oxygen

Test temperature	Tensile strength	Yield strength	Uniform elongation	Total elongation
22°C	24,000 psi	12,700 psi	27.3%	~ 40.7%
75	23,000	11,000	28.7	~ 44.7
125	21,600	9,400	26.1	35.6
150	22,600	9,650	22.4	32.9
175	21,800	9,700	20.1	29.6
200	22,300	9,400	22.4	33.0
225	21,600	8,750	19.8	29.3
275	26,900	8,700	14.8	21.9
325	34,700	9,700	17.7	26.4
350	36,800	12,200	16.4	25.4
375	34,800	11,300	14.9	22.6
400	34,500	9,700	16.0	26.4
425	32,700	10,250	13.1	~ 37.0
450	26,600	6,600	15.6	~ 49.0
500	23,100	---	---	~ 41.0

Table 20. Tensile properties of vanadium containing 265 ppm oxygen

Test temperature	Tensile strength	Yield strength	Uniform elongation	Strain hardening exponent
27°C	27,800 psi	16,200 psi	27.0%	0.240
121	23,600	11,700	30.2	---
147	25,100	---	24.6	0.283
165	24,200	11,050	24.7	0.324
188	24,200	11,500	23.0	0.301
212	26,000	---	23.1	0.334
243	29,600	11,050	16.6	0.399
273	33,200	10,500	19.9	0.457
300	34,900	11,600	16.8	0.433
350	35,900	13,700	16.5	0.441
379	37,200	13,100	20.9	0.485
401	38,600	12,800	14.9	0.484
453	30,900	8,350	14.5	0.425

Table 21. Tensile properties of vanadium containing 955 ppm oxygen

Test temperature	Tensile strength	Yield strength	Uniform elongation	Strain hardening exponent
24°C	45,200 psi	36,800 psi	10.8%	0.150
100	44,500	36,500	10.5	0.169
120	43,500	32,700	10.0	0.169
160	42,900	33,600	8.1	0.187
180	43,400	33,600	9.0	0.191
200	46,600	34,200	11.5	0.200
240	46,300	34,700	8.7	0.196
280	48,900	34,600	8.4	0.306
320	32,900	36,000	11.5	0.390
360	54,100	33,200	10.0	0.327
400	54,200	33,200	10.7	0.310
480	43,600	30,000	5.5	0.300

Table 22. Tensile properties of vanadium containing 1800 ppm oxygen

Test temperature	Tensile strength	Yield strength	Uniform elongation	Strain hardening exponent
27°C	59,800 psi	49,400 psi	14.6%	0.227
124	52,900	39,400	11.0	0.240
148	53,200	38,400	10.5	0.253
177	56,600	38,600	12.5	0.254
200	57,900	38,200	11.3	0.275
230	63,700	39,500	11.6	0.333
250	67,200	39,800	13.5	0.347
270	67,200	38,400	12.4	0.340
300	62,700	35,700	13.8	0.322
321	58,500	37,800	15.8	0.329
356	55,400	34,700	14.0	0.322
375	54,300	34,400	8.1	0.329
402	49,700	32,800	5.8	0.327

be due to the larger grain size, 16 grains/mm², of the sample containing the lowest amount of oxygen as compared with a grain size of 400 grains/mm² for the other samples. However, all the samples with less than 300 ppm oxygen have about the same ductility above room temperature. On the other hand, the maximum may be caused by the combination of the increase in strain hardening and a much lower hardness at very low oxygen concentrations.

The tensile properties of vanadium between room temperature and 500°C were studied in detail as a function of oxygen concentration. The tensile strength versus test temperature curves (Figure 13) show minima in the strength around 150° to 200°C and maxima around 350° to 400°C for most oxygen concentrations, although the maximum is shifted to about 250°C in the high-oxygen specimens. The maximum tensile

strength for all oxygen concentrations coincided with serrations in the stress-strain curves, a maximum in the yield strength, a maximum strain hardening exponent, and a minimum strain rate sensitivity. The minimum in the tensile strength was coincident with a minimum in the yield strength and serrations in the stress-strain curves for oxygen contents above 250 ppm.

The yield stresses shown in Figures 14 and 15 are the lower yield points or, if the sample had no yield point, the equivalent 0.2% offset yield strengths. The minima and maxima in the yield strength curves match the corresponding tensile strength curves, as mentioned before. The effect of temperature upon the strain hardening exponent (Figure 16) is similar in that the exponent increases to a maximum in the same temperature range, but it appears to be fairly constant above 400°C in most cases. The strain rate sensitivity m , defined by the equation $m = \left(\frac{\partial \log \sigma}{\partial \log \dot{\epsilon}} \right)_{\epsilon}$, was measured with vanadium containing 265 ppm oxygen, as shown in Figure 17, and a minimum was observed at about 375°C. The negative strain rate sensitivity signifies that vanadium in the 225° to 425°C range deforms at lower stress at high strain rates than at low strain rates, a phenomenon not reported for other body-centered cubic metals above room temperature.

Typical stress-strain curves are shown in Figure 18; the four curves for 1800 ppm oxygen were selected to show the two serration ranges for the metal, while those at 47 ppm oxygen illustrate the changes observed in the curves and in the serrations for low-oxygen vanadium. It should be noted that only the portions of the curves up to the maximum are

depicted, to conserve space, but all samples were ductile at all temperatures and necked down to a reduction in area of nearly 100%.

A graphical summary of the serrations observed in the tensile tests is given in Figure 19, in which the height of the serrations or the average width of the serration band is plotted as a function of temperature. These curves illustrate the two serration ranges observed:

- 1) in low-oxygen vanadium, serrations in the stress-strain curves are evident around 400°C and these serrations decrease in magnitude and are observed at a lower temperature as the oxygen content is increased;
- 2) above 300 ppm oxygen a second serration range appears around 150°C and increases with increasing oxygen content.

A study of the aging times at various temperatures required for the return of a ten-pound yield point (Table 23) showed a diffusion-controlled process with an activation energy of 27,700 calories per

Table 23. Aging treatments for tensile test yield point return (all experiments performed on the same sample of vanadium containing 265 ppm oxygen)

Aging temperature	Time for 10-pound yield point return
130°C	182 min.
143	59
150	34
168	9.5
187	2.6

The 10-pound yield point equals 812 psi for the 0.125 inch diameter sample.

gram-atom. This was determined graphically (Figure 20) by plotting the Napierian logarithm of the reciprocal of the aging time as a function of the reciprocal of the absolute temperature. From Fick's first law of diffusion, $J = -D \left(\frac{\partial c}{\partial x} \right)$, the diffusion coefficient can be expressed as $D = D_0 \exp (-Q/RT)$, where Q is the activation energy for diffusion and R is the gas constant. The concentration gradient is $-\left(\frac{\partial c}{\partial x} \right)$ and J is the flux, or the number of atoms which pass through a unit area in a unit time. The flux then must be inversely proportional to the time required for diffusion, or $J \propto 1/t \propto D \propto \exp (-Q/RT)$. This can be expressed as $\log_e 1/t + K = -Q/RT$. Consequently, the slope of the straight line obtained from a graph of $\log_e 1/t$ versus $1/T$ must be $-Q/R$. The activation energy for diffusion of carbon is 27,300 cal/g-atom so it seems likely that the strain aging effects observed in low-oxygen vanadium were caused by the interaction of both oxygen and carbon atoms with dislocations in vanadium.

The interaction energy between an oxygen atom and an edge dislocation in vanadium was calculated from the equation $T_o = \frac{V_{\max}}{k \log_e (1/c_o)}$, where c_o is the atomic concentration of solute and T_o is the temperature of the yield point disappearance (31), which is approximately 450°C for vanadium containing 740 ppm oxygen. The result, 0.37 eV for the interaction energy, is in good agreement with the value of 0.34 eV obtained from correction of the interaction energy of carbon and nitrogen in iron by the theoretical expression of Cottrell and Bilby (13).

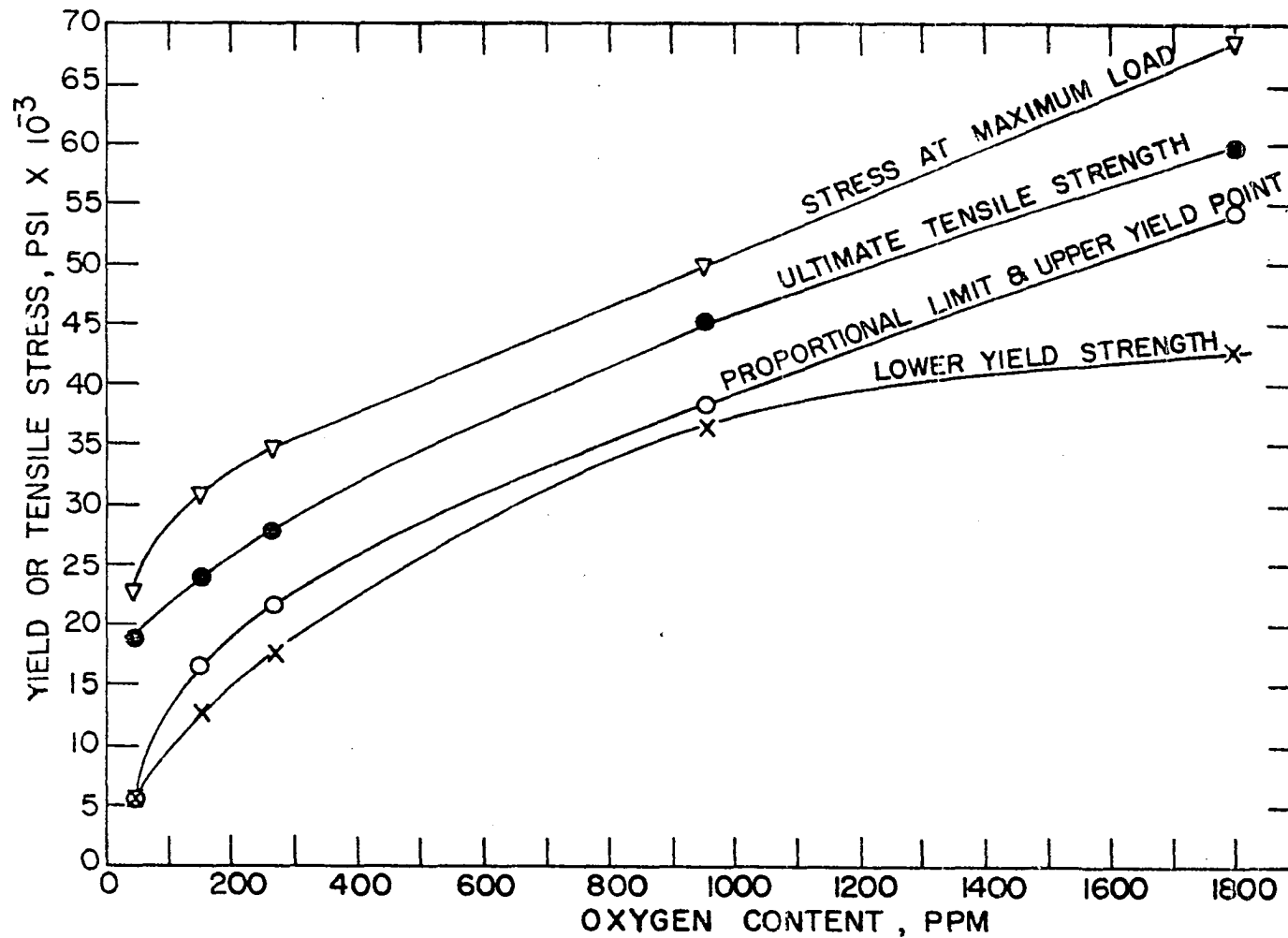


Figure 10. Effect of oxygen on tensile properties at room temperature

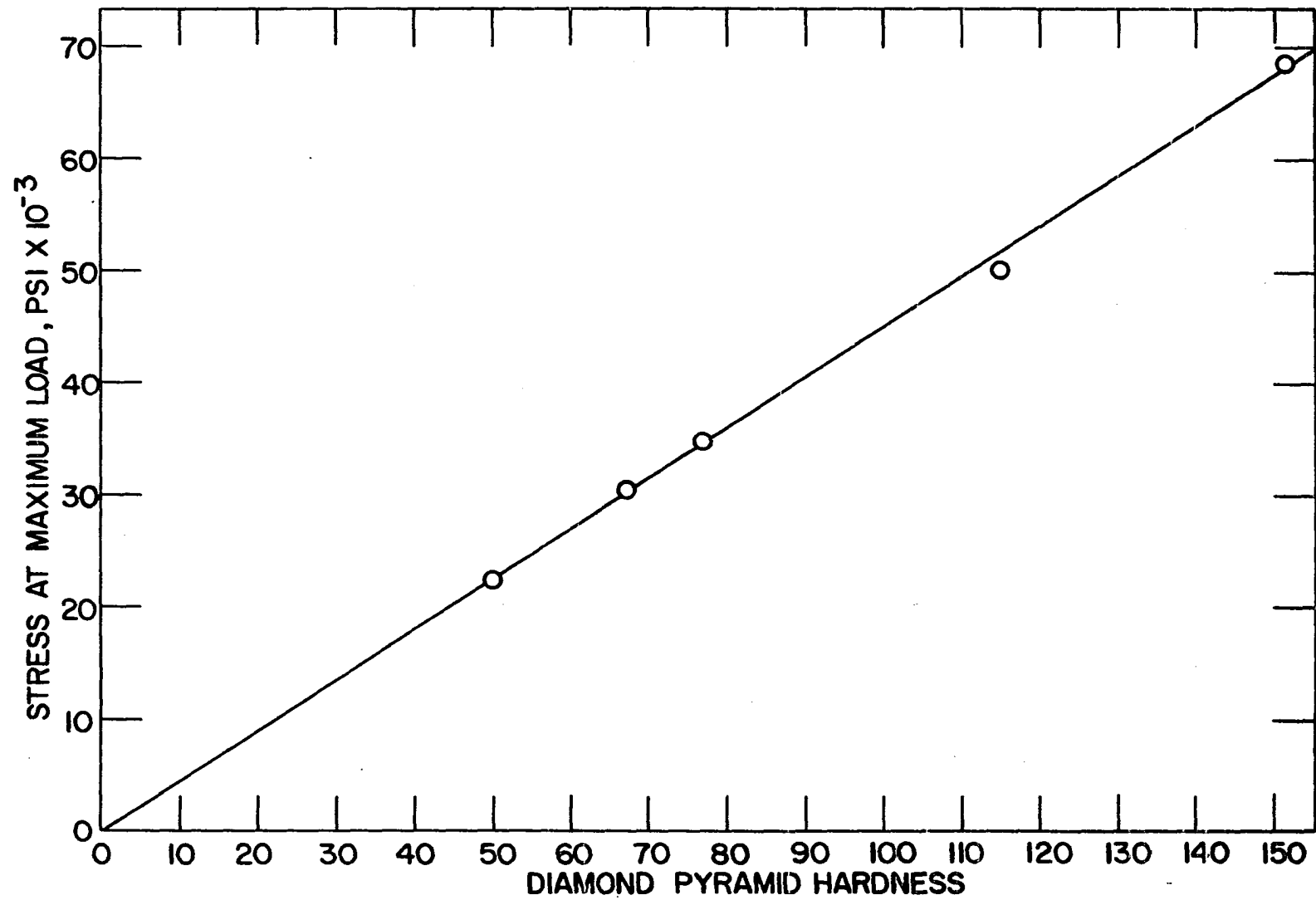


Figure 11. Relation of hardness and tensile stress at maximum load

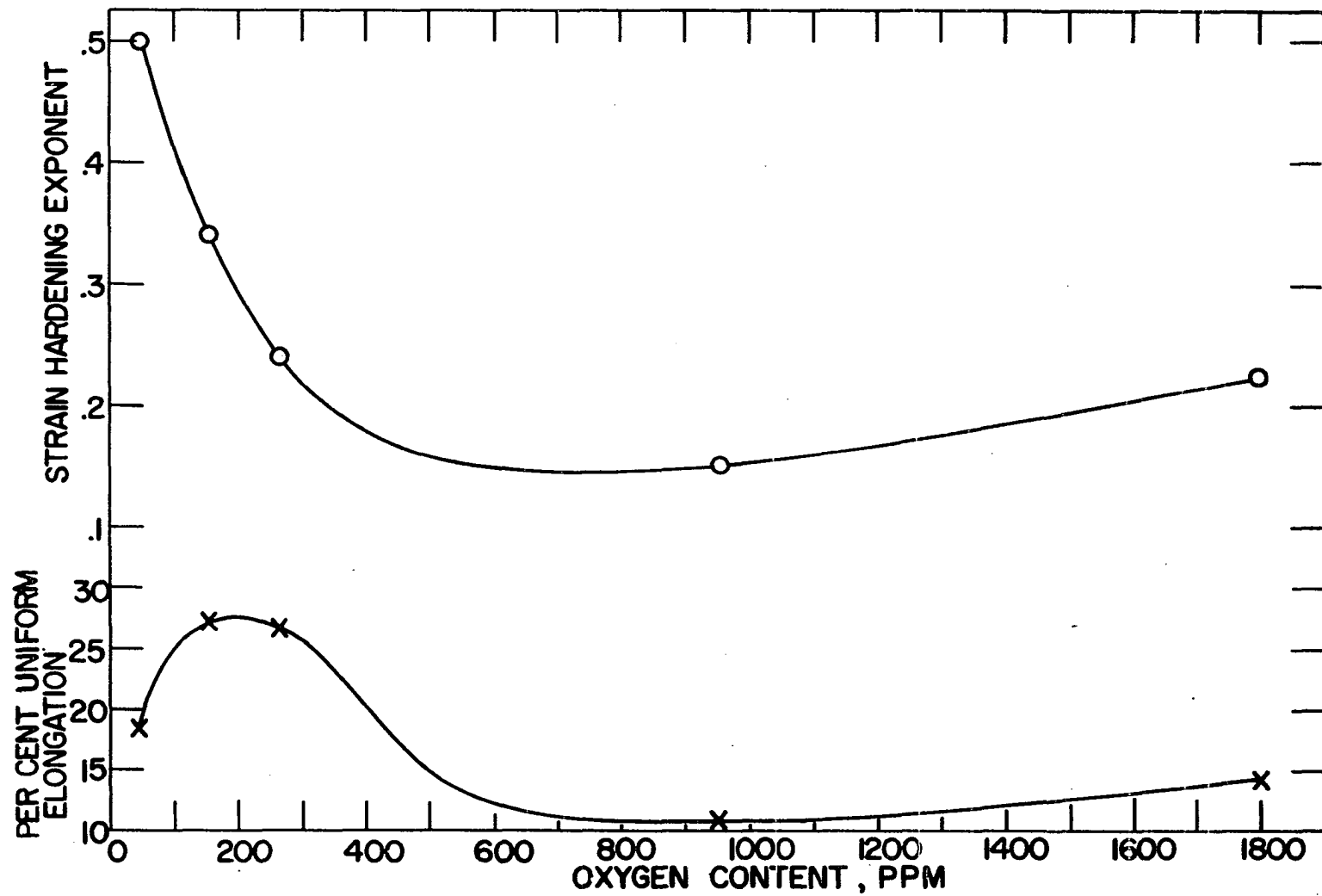


Figure 12. Strain hardening and elongation at room temperature

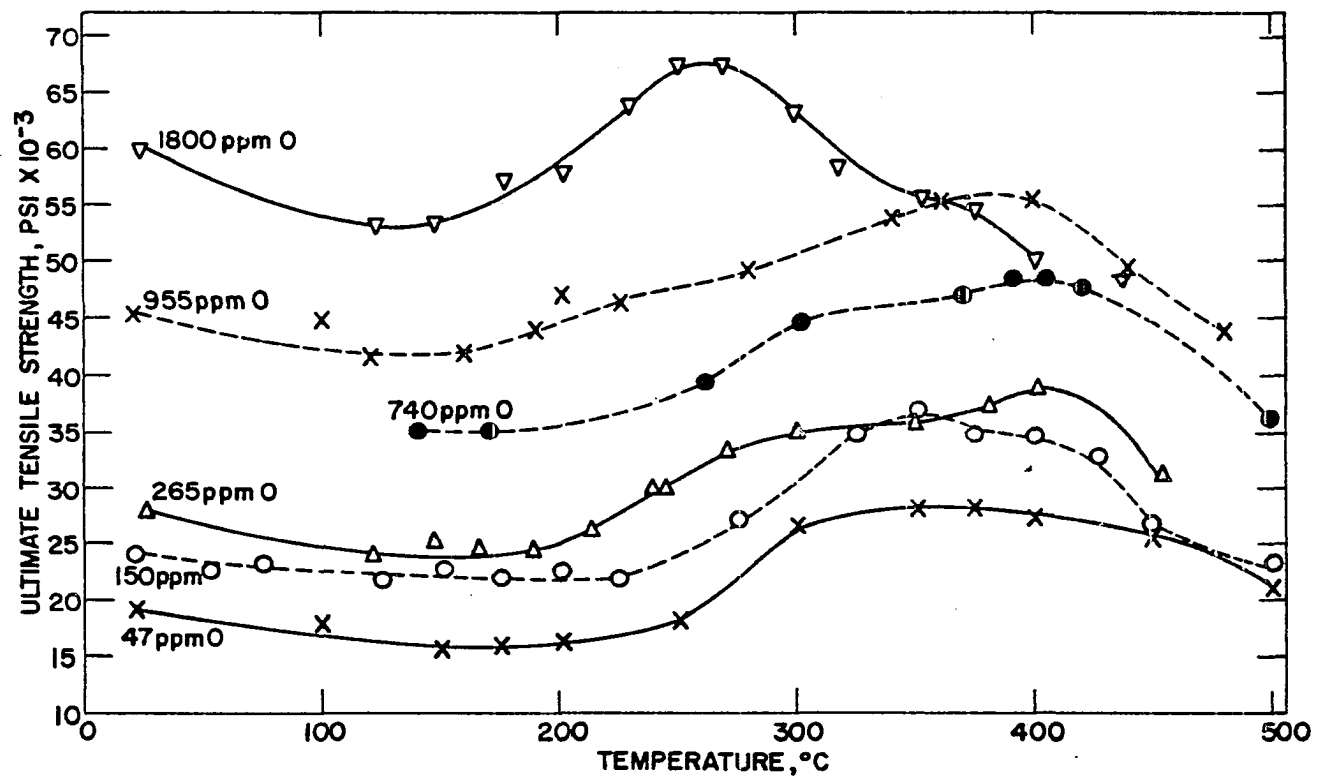


Figure 13. Variation of tensile strength with temperature

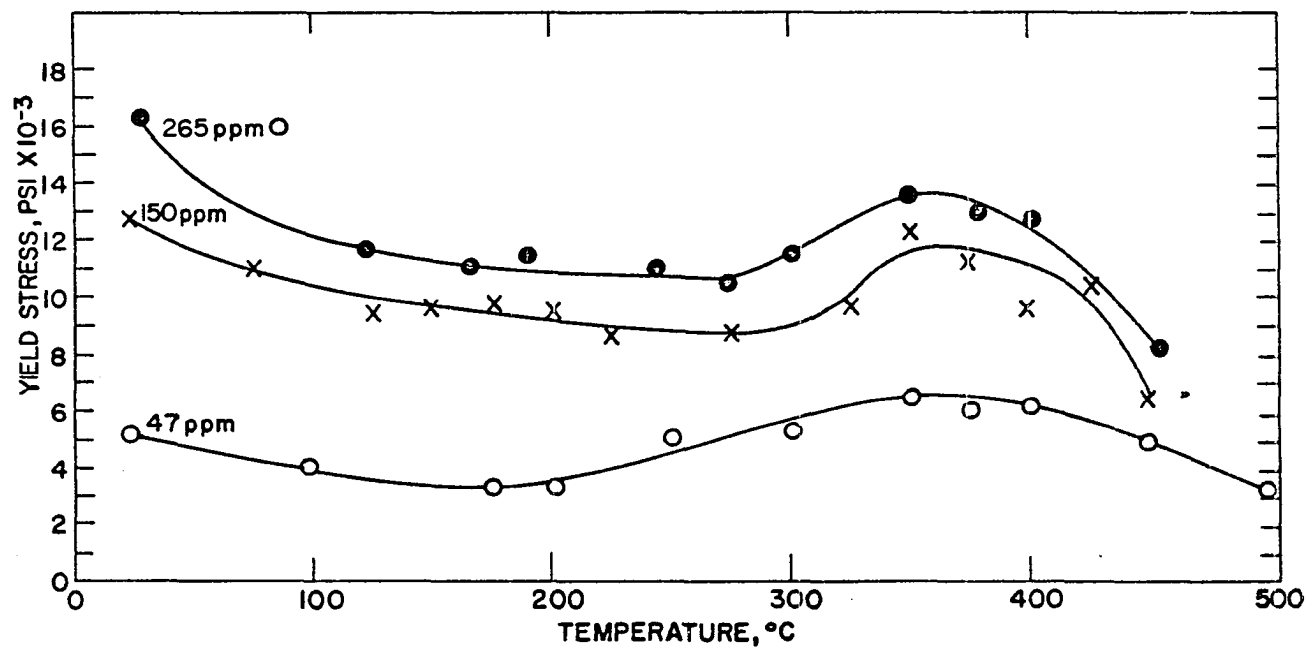


Figure 14. Variation of yield stress with temperature for low-oxygen vanadium

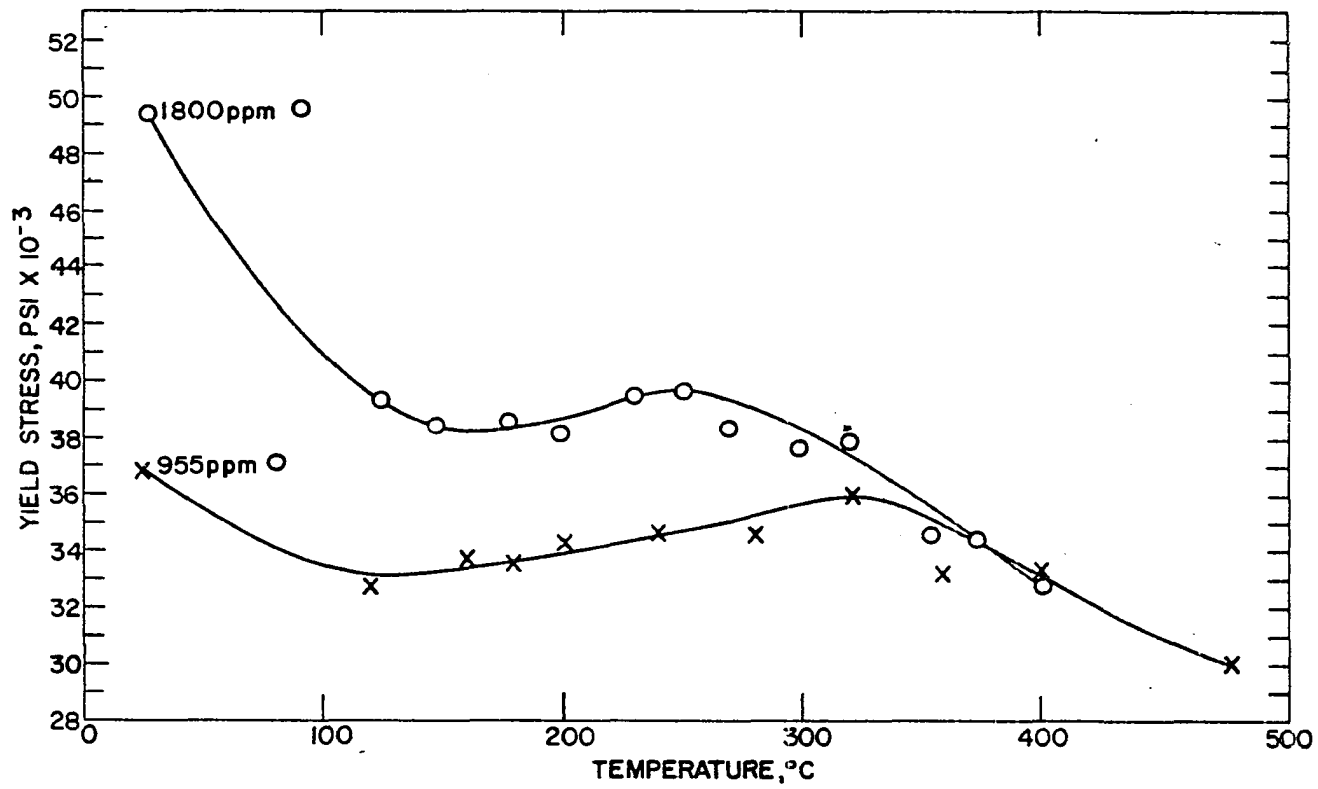


Figure 15. Variation of yield stress with temperature for high-oxygen vanadium

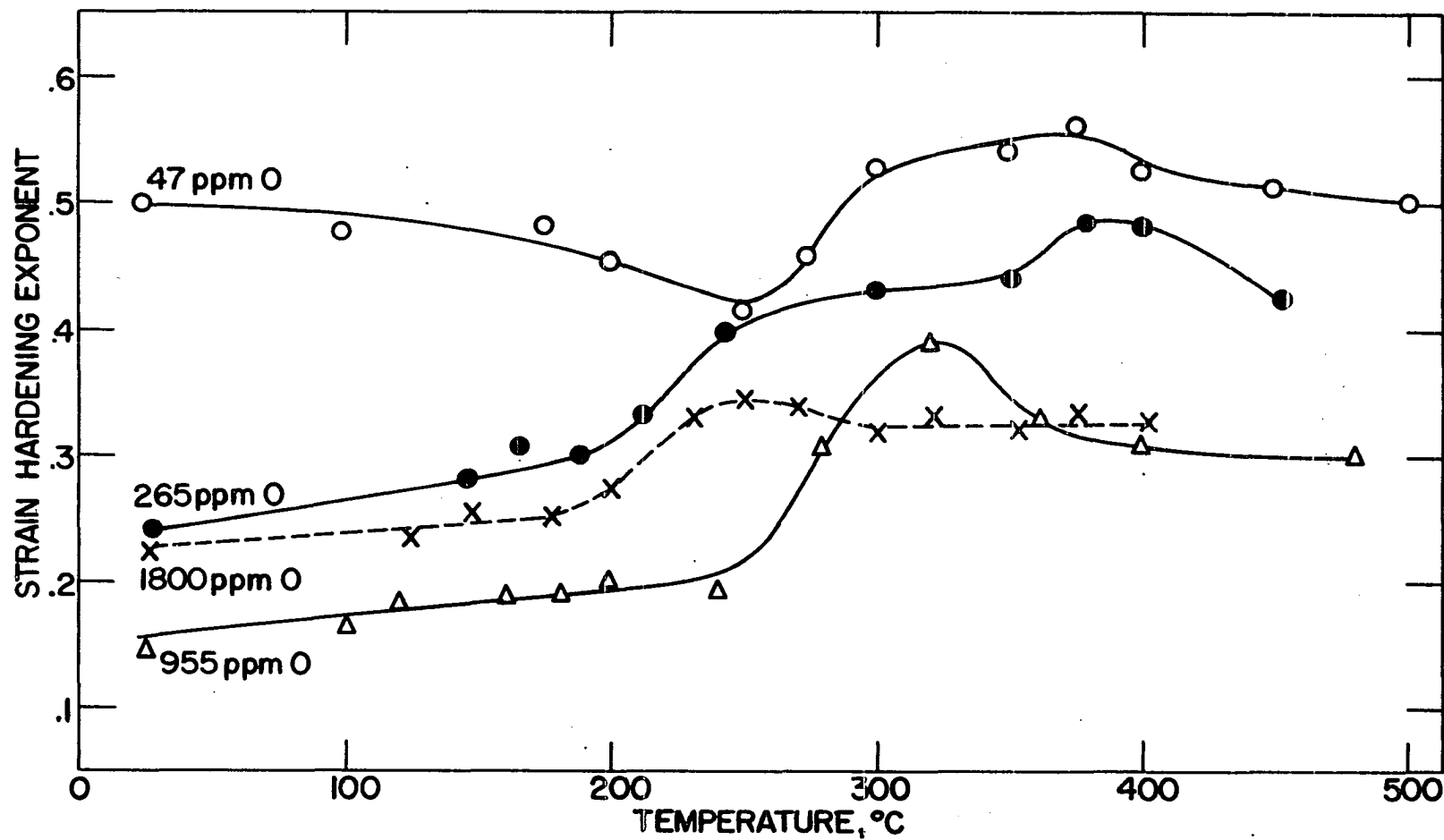


Figure 16. Effect of temperature on strain hardening of vanadium

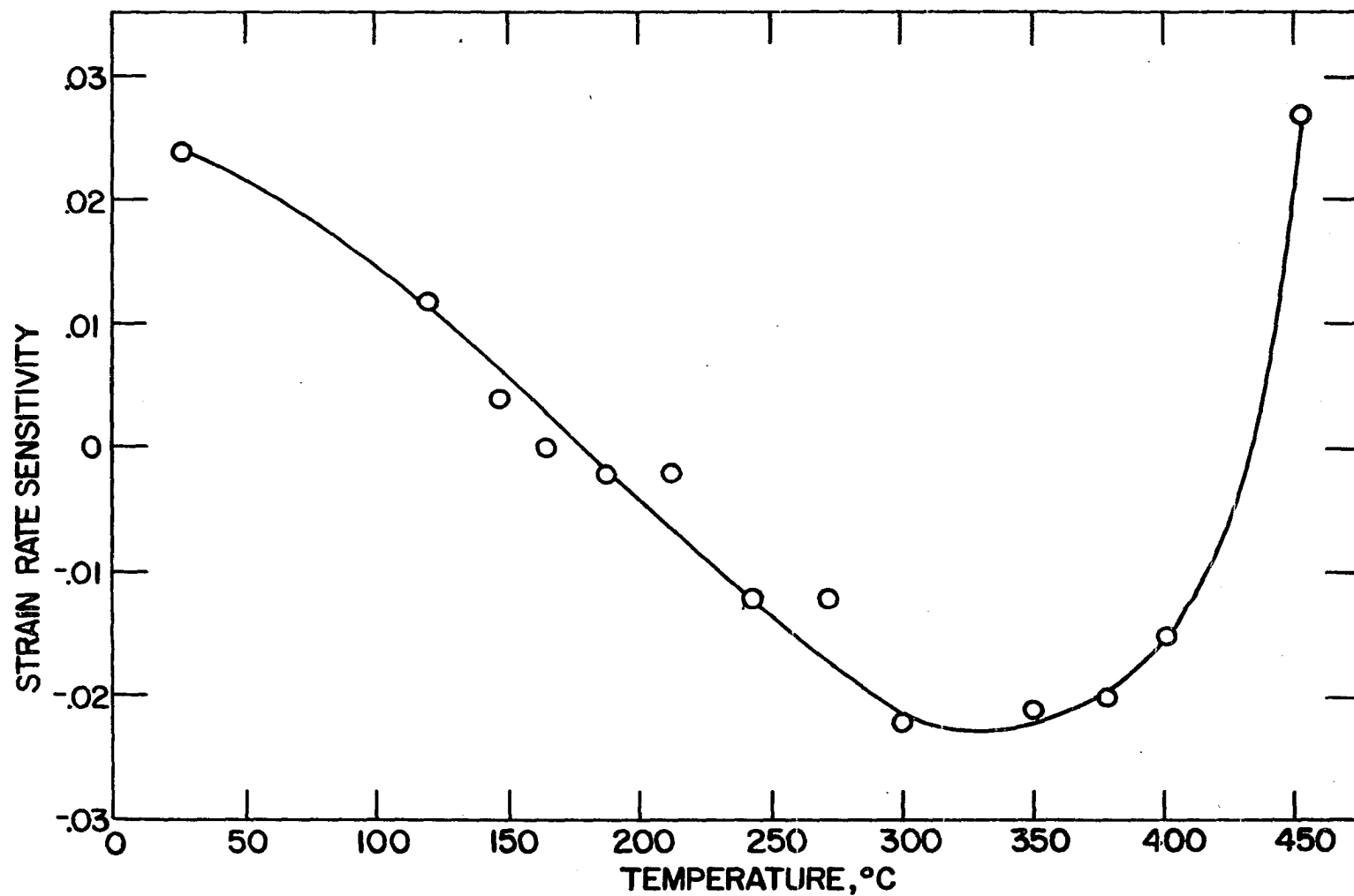


Figure 17. Strain rate sensitivity of vanadium containing 265 ppm oxygen

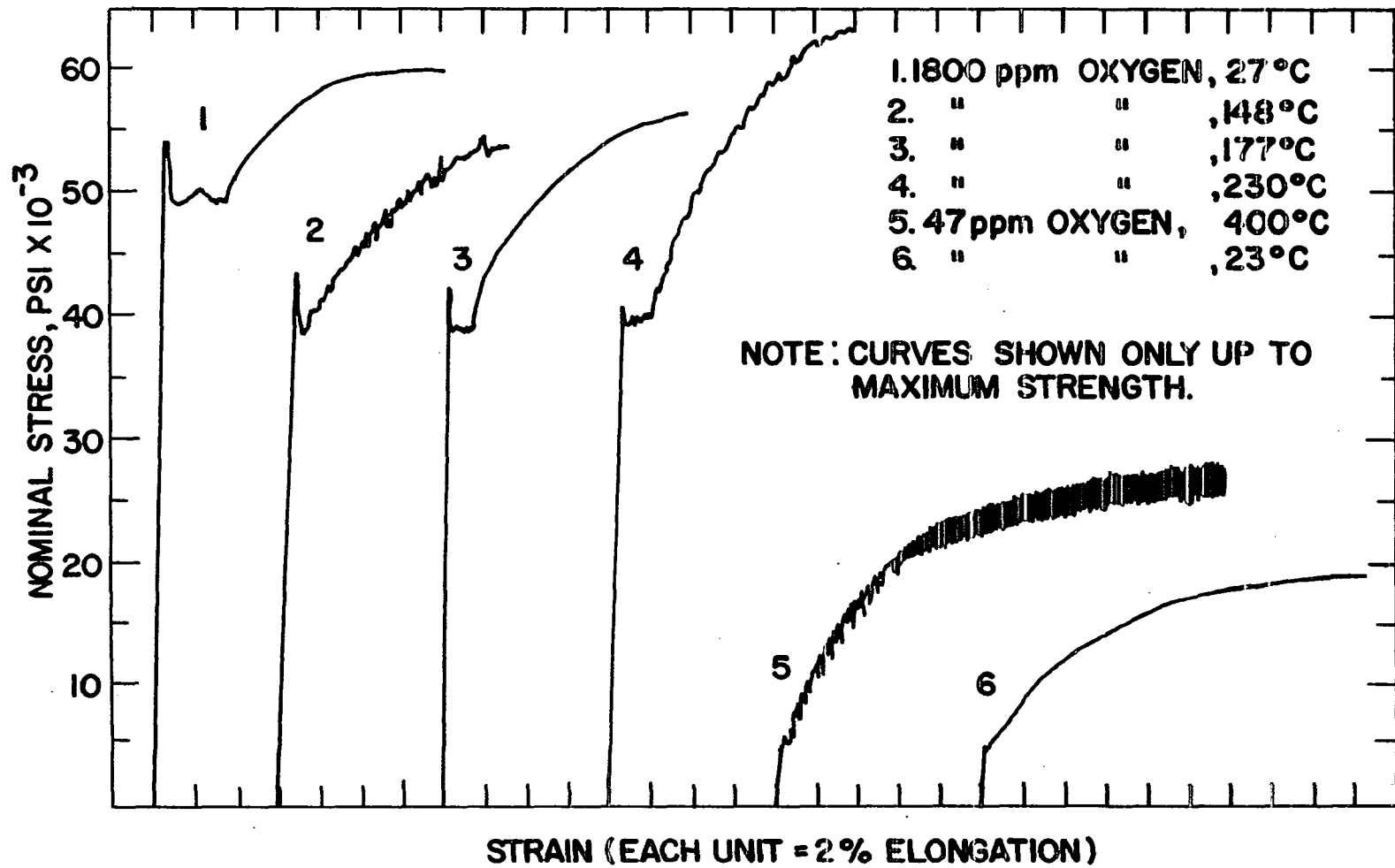


Figure 18. Typical stress-strain curves

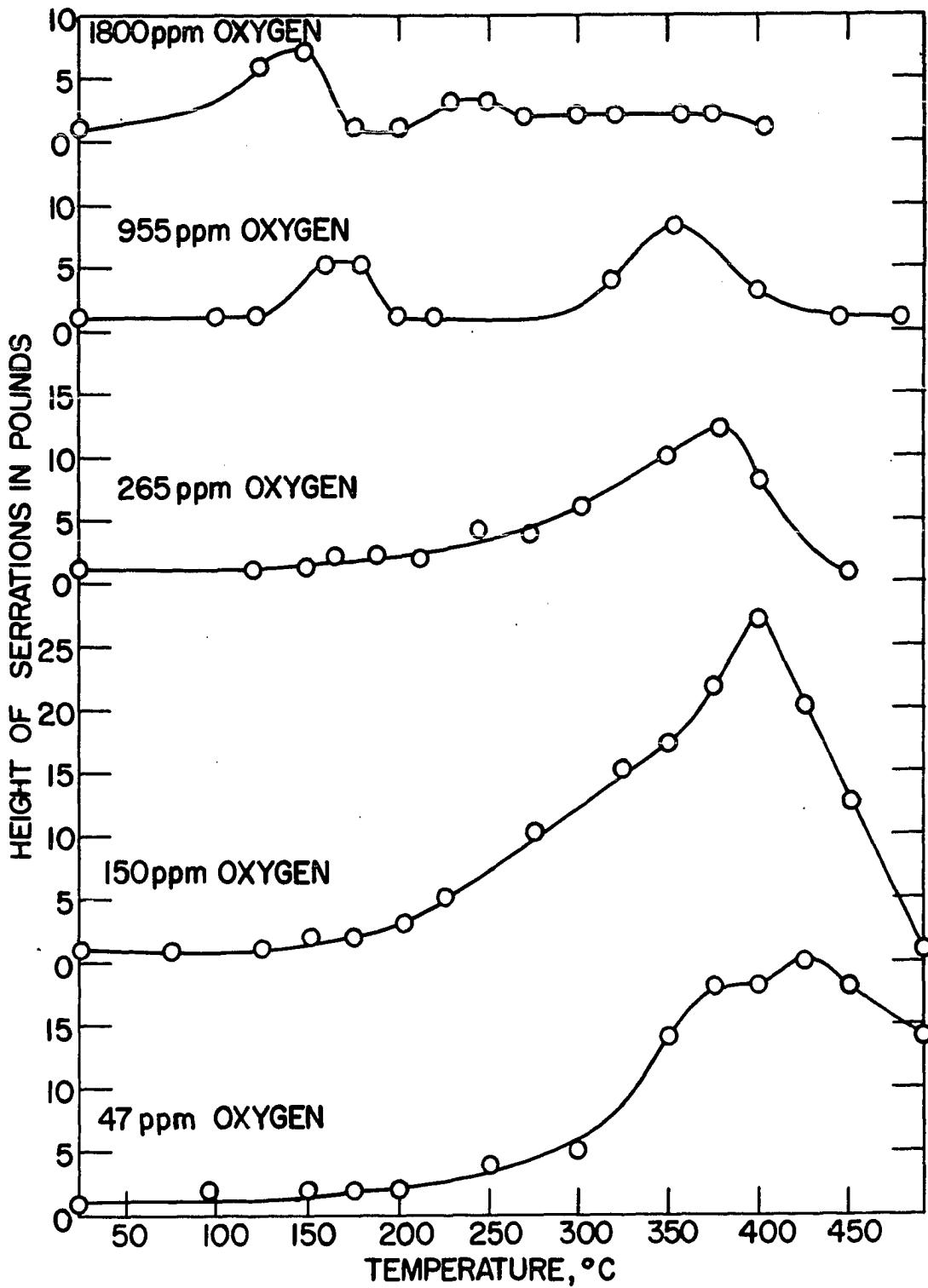


Figure 19. Serrations of tensile tests

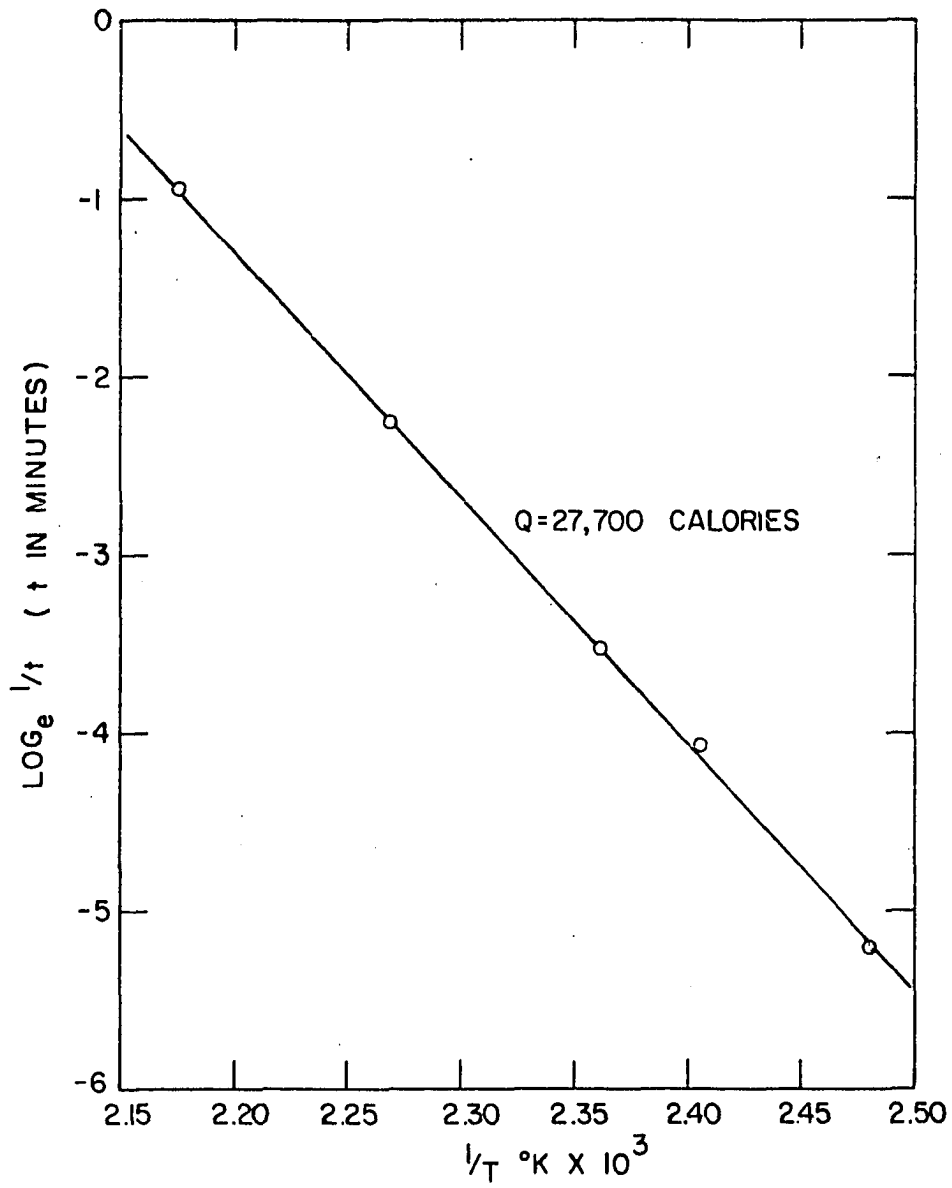


Figure 20. Activation energy for return of yield point

VI. DISCUSSION OF RESULTS

While much of the material in the previous section is self-explanatory, some observations on the lattice constant determinations, the bend tests, and the strain aging experiments are needed and will be given here. In addition, it will be shown how an expansion of Cottrell's theory of strain aging can be used to interpret the tensile tests of vanadium.

A. The Lattice Constant

The possibility of a tetragonal distortion of the vanadium lattice caused by solution of oxygen was investigated with the high-oxygen samples. No distortion was observed from the appearance of the diffraction pattern or by calculation of the lattice constant from the $\{hk0\}$ and $\{h00\}$ reflections. Klemm and Grimm (24) are alone in reporting the distortion, and their results were quite self-consistent, so it seems likely that the oxygen was not dissolved homogeneously throughout their vanadium.

An examination of lattice constants calculated from the 17 K α reflections, from $\theta = 58^\circ$ to $\theta = 83^\circ$, showed that Straumanis' criticism (49) of Cohen's extrapolation method (9) was justified; the lattice constants when plotted against $(\frac{\pi}{2} - \theta) \cot \theta$, or θ , or the Nelson-Riley function did not approximate a straight line sufficiently for accurate extrapolation. The lattice constants calculated from reflections at $\theta = 58^\circ$ to 65° are invariably too low, those from $\theta = 65^\circ$ to 75°

are erratic, and those from 75° to 83° are independent of the diffraction angle. Consequently an average of the three strong $K\alpha_1$ reflections from $\theta = 75^{\circ}$ to 83° appears best for accurate lattice constant determination of vanadium when molybdenum radiation is used in the back reflection camera.

The discrepancy between the lattice parameter of 3.0240 \AA found by James and Straumanis (20) and the value of 3.0259 \AA obtained in this investigation is not readily explainable. The vanadium which they used contained 0.005 w/o carbon, 0.002 w/o nitrogen, and 0.015 w/o oxygen, which differed chiefly in its lower carbon content from the metal in this study, although both were obtained by the iodide crystal-bar process. Since carbon apparently has very little effect on the lattice constant when present in concentrations from 0.010 w/o to 0.045 w/o it is possible that carbon has a solubility of less than 0.010 w/o at 900°C and has a much greater effect on the lattice parameter than oxygen when it is in solid solution, but these propositions remain to be substantiated.

James and Straumanis calculated their lattice constants from the $K\alpha_1$ (321) reflection from copper radiation upon the assumption that at high diffraction angles (72° in this case) the lattice constant is essentially independent of the angle. If the assumption is not completely valid a lattice parameter obtained by this method would be too small. Patterns taken in the back-reflection focusing camera with unfiltered copper radiation show two distinct lines at higher diffraction angles which should be better for calculation: the $K\alpha_2$ (321) reflection at 73° and the $K\beta$ reflection of the (411) and (330) planes at 78° .

The lattice parameter of $3.0258 \pm 0.0001 \text{ \AA}$ obtained by Seybolt and Sumsion for crystal-bar vanadium is in reasonably good agreement with the constant of 3.0259 \AA determined in this study. Back-reflection focusing cameras were used for both measurements, while smaller Debye-Scherrer cameras were used by James and Straumanis (20) and by Gurevich and Ormont (17) to obtain a constant of 3.0240 \AA , and a diffractometer was used by Loomis and Carlson (27) to get a lattice constant of 3.023 \AA for crystal-bar vanadium.

B. Mechanical Strength and Embrittlement

Louat and Wain (28) have explained the relationship between the yield stress and temperature shown in Figure 7 on the basis of dislocation locking by solute atoms in two different energy levels near the centers of the dislocations. From their derived equations they were able to predict a temperature range in which the yield stress was proportional to $1/T$, and a still lower range in which it was approximately invariant with T . The secondary atmosphere lying outside the central region of the dislocation was noted as having an influence by reducing the stress field, and thereby the interaction energy, at the center of the dislocation.

The variation of yield stress with temperature, as illustrated in Figure 7, has also been observed with Ta, Cr, W, Mo, and Fe, among others, and fits the theory of Louat and Wain very well. An extension of the work to explain the similar behavior of the maximum stress, shown in

Figure 8, has not yet been made but the two would appear to be closely related.

The fracture loads for brittle samples were not generally plotted in Figures 7 and 8, inasmuch as the bend test load, unlike the tensile stress, does not indicate the load necessary to propagate a crack through a brittle sample. Crack propagation in a bend test can take place under a reduced load because of the geometry of the test so that the maximum load in a brittle bend test is the load required to initiate the crack.

The results of the present study of embrittlement of vanadium by oxygen were not expected since Loomis and Carlson (27) found that the addition of 1000 ppm oxygen to calcium-reduced vanadium raised the brittle-ductile transition temperature nearly 100°C . This work on high-purity vanadium, however, has shown that addition of $0.15\text{ }^{\text{w}}/\text{o}$ oxygen does not embrittle vanadium above -196°C , although it nearly triples the Diamond Pyramid Hardness and tensile strength, and increases the yield strength by a factor of about 9 at room temperature. The practical possibilities in such an alloy may be worth further study. If the calcium-reduced vanadium tested by Loomis and Carlson is assumed to have had an oxygen content of 0.20% , the results of these two studies agree.

C. Strain Aging

There are several phenomena observed in vanadium tensile tests between 25° and 500°C indicating the presence of a strain aging mechanism which does not appear to be explained completely by the usual

interpretation of the dislocation locking theory of Cottrell (12). The results of this investigation suggest that a more complete picture of strain aging as applied to vanadium might be as follows:

In tensile tests at slow strain rates and at low temperatures the solute atoms do not have enough mobility to diffuse to the slowly-moving dislocations. At approximately 150°C for vanadium strained at 0.01 inch per minute, it is proposed that the diffusion rate of oxygen has increased to the point that oxygen atoms can catch the dislocations and momentarily lock them, which causes serrations in the tensile curve. As the temperature increases, the oxygen should be able to diffuse along with the dislocations, creating a drag on them but no longer locking them. When the temperature approaches the temperature of the yield point disappearance (approximately 450°C for vanadium containing 740 ppm oxygen) the oxygen, which has been in a condensed line along the dislocation, begins diffusing to a dilute atmosphere around the dislocation. This secondary atmosphere weakens the interaction between the condensed atmosphere and the dislocation. Consequently, it is submitted that the dislocations should again be able to pull free of the solute atoms, causing a second serration range. At still higher temperatures there are no condensed atmospheres at the dislocations and the effect of the solute atoms becomes negligible.

Using this explanation of the interaction between solute atoms and dislocations the author believes that the strain aging effects in vanadium can be logically interpreted. The observations are enumerated below and then discussed in detail.

1. There are two temperature ranges in which multiple serrations appear in the stress-strain curves. The appearance of the serrations in the two ranges is different: serrations in the lower range appear to be a momentary rise in stress while those in the upper range are a momentary drop in stress.

It is proposed that the serrations in the low-temperature range are caused by the momentary locking of free dislocations by solute atoms, thereby increasing the stress. Serrations in the high-temperature range are believed to be caused by the momentary release of dislocations from their atmospheric drag, thereby decreasing the stress.

2. In the lower temperature range the frequency and height of the serrations decrease with decreasing oxygen concentrations, disappearing below 300 ppm oxygen; in the upper range the serrations decrease with increasing oxygen concentration, disappearing at about 2000 ppm oxygen but persisting at a concentration of 47 ppm. Increasing the oxygen concentration depresses both serration temperature ranges.

The relation of the serrations to oxygen content suggests that the low-temperature serrations depend upon sufficient oxygen diffusing to the slowly-moving dislocations to lock them. As the oxygen concentration decreases, the distance of diffusion increases so that fewer oxygen atoms reach the dislocations. At high oxygen concentrations the number of oxygen atoms necessary for pinning reaches the dislocations at a lower temperature to start the multiple yielding. The high-temperature serrations, however, should decrease as the oxygen atmospheres around the dislocations increase and make escape more difficult. Higher oxygen

concentration allows a larger diffuse atmosphere to form and the atmosphere starts forming at a lower temperature to begin the serrations.

3. The lower serration region is accompanied by a minimum tensile strength and the upper serration range occurs around the maximum tensile strength, the difference between the minimum and maximum strengths being constant for all oxygen concentrations from 150 to 1800 ppm.

It is postulated that the minimum strength occurs at a temperature at which dislocations have a much greater mobility than oxygen. There is almost no drag on the dislocations; they are either locked or free. The maximum in strength is presumed to occur when the drag on the dislocations offered by oxygen atoms in the condensed atmosphere is a maximum, while above this temperature the diffusion of oxygen to form the secondary atmosphere reduces the drag on the dislocations by reducing the stress fields at the centers of the dislocations. The increase in strength should be the result of resistance to motion of the dislocations, due primarily to the presence of oxygen atoms in condensed atmospheres at the dislocations. This ought to be essentially independent of the oxygen concentration in the rest of the metal.

4. The strain rate sensitivity is a minimum (negative) and the strain hardening exponent is a maximum in the higher temperature serration range.

In the strain aging temperature range an increase in the velocity of dislocations by an increase in strain rate will reduce the number of oxygen atoms which can diffuse to the dislocations. A smaller atmosphere creates less drag and results in a lower stress. The strain

hardening increases as the lowest-energy positions at the dislocations are being filled with oxygen atoms. When oxygen starts occupying the higher-energy positions in the area around the dislocations (the secondary atmosphere), the strain hardening decreases.

5. The greater the yield point drop the greater the serrations in the higher temperature range. Above about 400°C both the yield point and the serrations disappear, as predicted by Mott (31).

The yield point and the upper-range serrations should be alike in having oxygen atoms in positions of lowest energy at the dislocations and also as a secondary atmosphere. A large yield point drop and deep serrations are the result of long movements of free dislocations.

6. Below 200°C , aging in the absence of a load gives a yield point return and aging under a constant load reduces the time required for yield point return. However, for a tensile test carried out in the high-temperature serration range, interruption of the test for an aging period causes yielding at a lower stress, and no yield point, when the tensile test is resumed. If the tensile test is carried out at room temperature and the sample aged in the 350° to 400°C temperature range, a yield point is observed when the test is resumed. As explained in the previous section, the activation energy for the yield point return is 27,700 cal/g-atom.

At low temperatures, aging should increase the amount of oxygen which diffuses to the dislocations to lock them. With a load imposed, the stress in the metal assists diffusion of oxygen to lock the dislocations. At high temperatures, aging during the tensile test should

increase the secondary atmosphere, thereby reducing the stress required to move the dislocations. In tensile tests at room temperature, however, aging allows oxygen to diffuse to form condensed atmospheres at free dislocations, raising the stress in the metal.

The activation energy of 27,700 calories per gram-atom found for the yield point return after aging of vanadium between 130° and 190°C is within 3% of the average of the internal friction results and the stress-relaxation measurement for the diffusion of oxygen in vanadium.

VII. SUMMARY AND CONCLUSIONS

The effect of 47 to 3100 ppm oxygen in vanadium has been investigated by x-ray measurements, low-temperature bend tests, hardness tests, and tensile tests from 22°C to 500°C. The important observations, and the conclusions which can be drawn from them, are given below:

1. The lattice constant of crystal-bar vanadium extrapolated to 0% oxygen is 3.0259 ± 0.0002 Å. Oxygen increases the lattice constant of vanadium by 1.5×10^{-6} Å/ppm.
2. Oxygen does not embrittle vanadium above -196°C if present in amounts less than 0.15%. Embrittlement does occur for greater concentrations; for example, vanadium containing 0.25% oxygen has a brittle-ductile transition temperature of -90°C.
3. Strain aging behavior is observed in two separate temperature ranges in tensile tests of high-oxygen vanadium at slow strain rates. The activation energy for return of the yield point is 27,700 cal/g-atom, which is approximately the same as for diffusion of oxygen in vanadium.
4. It is proposed that strain aging can occur in two steps: first, the locking of dislocations by interstitial impurities in a condensed atmosphere, and second, at higher temperatures, the diffusion of the interstitial atoms to form a dilute atmosphere around the dislocations. Each step is accompanied by serrations in the stress-strain curves.

VIII. BIBLIOGRAPHY

1. Allen, N. P., Kubaschewski, O., and Goldbeck, O. von. J. Electrochem. Soc. 98: 417. 1951.
2. Baker, D. H. and Ramsdell, J. D. J. Electrochem. Soc. 107: 985. 1960.
3. Barrett, Charles Sanborn. Structure of metals. New York, McGraw-Hill Book Co. 1952.
4. Beatty, S. J. Metals. 4: 987. 1952.
5. Brown, C. M. Mechanical properties of high purity vanadium. Paper presented at Electrochemical Society meeting, New York, April 16, 1953. (Original not available for examination; reported in Hampel, Clifford A., ed. Rare metals handbook. pp. 594-596. New York, Reinhold Publishing Corp. 1954.)
6. Bullough, R. and Newman, R. C. Proc. Roy. Soc. (London). Ser. A, 249: 427. 1959.
7. Carlson, O. N. and Owen, C. V. J. Electrochem. Soc. 108: 88. 1961.
8. Clough, W. R. and Pavlovic, A. S. Trans. Amer. Soc. Metals. 52: 948. 1960.
9. Cohen, M. U. Rev. Sci. Instr. 6: 68. 1935.
10. Cottrell, A. H. Dislocations and plastic flow in crystals. Oxford, England, Oxford University Press. 1953.
11. _____. Phil. Mag. 44: 829. 1953.
12. _____. Progr. in Metal Phys. 4: 205. 1953.
13. _____ and Bilby, B. A. Proc. Phys. Soc. (London). Ser. A, 62: 49. 1949.
14. _____, Hunter, S. C., and Nabarro, F. R. N. Phil. Mag. 44: 1064. 1953.
15. _____ and Jaswon, M. A. Proc. Roy. Soc. (London). Ser. A, 199: 104. 1949.
16. Eustice, A. L. and Carlson, O. N. Trans. Am. Inst. Mining Met. Engrs. 221: 238. 1961.

17. Gurevich, M. A. and Ormont, B. F. Fiz. Metal. i Metalloved. 4, No. 1: 112. 1957. (Original not available for examination; translated in Physics of Metals and Metallography. 4, No. 1: 88. 1957.)
18. Harper, S. Phys. Rev. 83: 709. 1951.
19. Ingram, A. G. U. S. Atomic Energy Commission Report DMIC-134 [Battelle Memorial Inst. Defense Metals Information Center, Columbus, Ohio] . August 12, 1960.
20. James, William J. and Straumanis, M. E. [To be published in Z. physik. Chem. (Frankfurt), 1961].
21. Jordan, Charles B. and Duwez, Pol. Trans. Amer. Soc. Metals. 48: 783. 1956.
22. Ketelaar, J. A. A. [Unpublished work at the Leiden Institute for Inorganic Chemistry, Leiden, Netherlands.] (Original not available for examination; cited in Arkel, A. E. van. Reine Metalle. p. 224. Berlin, Julius Springer. 1939.)
23. Kirschfeld, L. and Sieverts, A. Z. Electrochem. 36: 123. 1930.
24. Klemm, Wilhelm and Grimm, Ludwig. Z. anorg. u. allgem. Chem. 250: 42. 1942.
25. Lacy, C. E. and Beck, C. J. Trans. Amer. Soc. Metals. 48: 579. 1956.
26. Lange, Norbert Adolph. Handbook of chemistry. 9th ed. Sandusky, Ohio, Handbook Publishers, Inc. 1956.
27. Loomis, B. A. and Carlson, O. N. Investigation of the brittle-ductile transition in vanadium. In Clough, W. R., ed. Reactive metals, vol. 2. pp. 227-243. New York, Interscience Publishers, Inc. 1959.
28. Louat, N. and Wain, H. L. Brittle fracture and the yield-point phenomenon. In Averbach, B. L., Felbeck, D. K., Hahn, G. T., and Thomas, D. A., eds. Fracture. pp. 161-180. New York, John Wiley and Sons, Inc. 1959.
29. Lyman, Taylor, ed. Metals handbook. 8th ed. Novelty, Ohio. American Society for Metals. 1961.

30. Mallett, M. W. and Bridge, J. R. [Unpublished work at Battelle Memorial Institute, Columbus, Ohio.] (Original not available for examination; cited in Rostoker, William. The metallurgy of vanadium. p. 20. New York, John Wiley and Sons, Inc. 1958.)
31. Mott, N. F. Mechanical strength and creep in metals. In Shockley, W., Hollomon, J. H., Maurer, R., and Seitz, F., eds. Imperfections in nearly perfect crystals. pp. 173-196. New York, John Wiley and Sons, Inc. 1952.
32. Nabarro, F. R. N. Mechanical effects of carbon in iron. In Report of a Conference on Strength of Solids, University of Bristol, July 7-9, 1947. pp. 38-45. London, The Physical Society. 1948.
33. Nash, Julian W., Ogden, H. R., Durtschi, Richard E., and Campbell, I. E. J. Electrochem. Soc. 100: 272. 1953.
34. Neuburger, M. C. Z. Krist. 93: 314. 1936.
35. Powers, R. W. Acta Met. 2: 604. 1954.
36. _____ and Doyle, Margaret V. Acta Met. 6: 643. 1958.
37. Pugh, J. W. General Electric Research Laboratory Report No. 56-RL-1532. April, 1956.
38. _____. Trans. Am. Inst. Mining Met. Engrs. 209: 1243. 1957.
39. Rostoker, William. The metallurgy of vanadium. New York, John Wiley and Sons, Inc. 1958.
40. _____, McPherson, D. J., and Hansen, M. Wright Air Development Center Technical Report 52-145, Part 2. 1954.
41. _____ and Yamamoto, A. S. Trans. Amer. Soc. Metals. 46: 1136. 1954.
42. _____ and _____. Trans. Amer. Soc. Metals. 47: 1002. 1955.
43. _____, _____, and Riley, R. E. Trans. Amer. Soc. Metals. 48: 560. 1956.
44. Schönberg, Nils. Acta Chem. Scand. 8: 624. 1954.
45. Seybolt, A. U. and Sumsion, H. T. J. Metals. 5: 292. 1953.

46. Smith, Karl F. Development of vanadium alloys for reactor application. Part 1. Evaluation. In Clough, W. R., ed. Reactive metals, vol. 2. pp. 403-414. New York, Interscience Publishers, Inc. 1959.
47. Smithells, Colin J. Metals reference book, vol. 1. 2nd ed. New York, Interscience Publishers, Inc. 1955.
48. Stanley, J. T. and Wert, C. A. Acta Met. 3: 107. 1955.
49. Straumanis, M. E. J. Appl. Physics. 30: 1965. 1959.
50. Tammann, G. and Schönert, K. Z. anorg. u. allgem. Chem. 122: 128. 1922.
51. Tichelaar, G. W., Coleman, R. V., and Lazarus, D. U. S. Atomic Energy Commission Report TID-11303 [Technical Information Service Extension, AEC]. July, 1960.

IX. ACKNOWLEDGMENTS

The author would like to express his thanks to C. V. Owen for the vanadium used in this investigation, to J. W. Hurd and W. Dallmann for the analytical determinations, and to L. K. Reed for assistance in the preparation of samples. The guidance and criticism by Dr. O. N. Carlson have been primarily responsible for the success of this study.